Vol 33 No. 2 Apr - Jun 2017 ISSN 0970-5953

PHYSICS EDUCATION

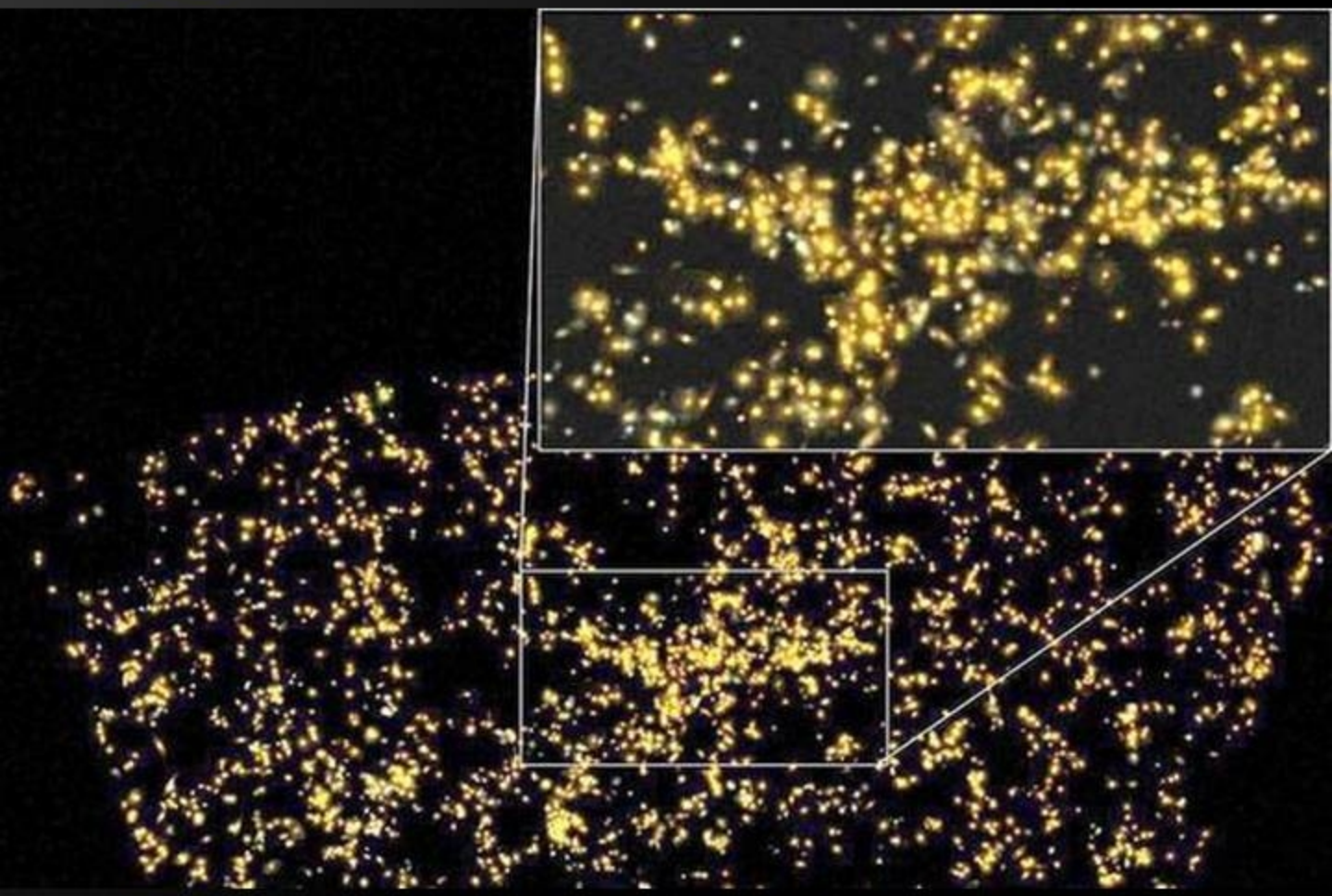

SARASWATI IN THE SKY

www.physedu.in

Volume 33, Number 2

In this Issue

EDITORIAL

As we promised earlier, this issue of *Physics Education* is accompanied by major changes in the website, including redesign and also backend processes related to editorial processing.

In particular, a new feature *web specials* has been introduced as a forum for informed debates about matters concerning any aspect of physics and its interface with other sciences and society. In this series, some of the first few articles deal with eclectic mix of physics related topics. Nilanjan Chaudhary discusses the motivations for theater version of the differences between two physicists of repute, namely, S. Chandrasekhar and Arthur Eddington. Sam Pitroda reflects about what physics taught him. R. Rangarajan dicusses ideas for making physics attractive for the next generation of students. Partha Ghose gives us a glimpse of what went on during a meeting between Einstein and Rabindranath Tagore in 1930. In the coming weeks and months, we hope we will have lively discussions around human and social dimensions of physics. The *web specials* section will be more dynamic and the content will change at least once every three weeks.

As we step in to the new redesigned website, we are also making small changes to how the manuscripts are handled. From 2018 onwards, all the manuscripts will have to be composed using latex word processing software. Latex has become the standard all over the world for producing publication quality output. However, we do not want to disappoint authors who are still using ms-word software. We might try out best to accommodate them and provide alternative facilities, but I can assure you that this change is for the better and will ensure much better quality look-and-feel for *Physics Education* pages. We seek the cooperation of the authors in order to implement this change.

Finally, as we had to implement these changes, this issue of *Physics Education* has been delayed by about two weeks. This will not repeat again. On behalf of the editorial and advisory board of *Physics Education*, I thank all the authors and readers for their continued support and for making this a relevant and worthwhile exercise.

M. S. Santhanam
Chief Editor
Physics Education

Ground state Energy Spectrum of One-Dimensional Pure Quantum Anharmonic Oscillators using Variation Principle

Shivalingaswamy. T[1*], Vanaja J. P.[1], Hemavathi S.[1],
Kavya J. [1], Gururaja H.S[1]

[1]P.G Department of Physics,
Govt. College (autonomous),
Mandya-571401, India.

[*]Corresponding Author: tssphy@gmail.com

(*Submitted*: 02-05-2017)

Abstract

We use Rayleigh-Ritz variational method to calculate the ground state energy eigenvalues of pure quantum anharmonic oscillators using appropriate asymptotic wave functions suggested by Ginsberg and Montroll, which requires a simple mathematical calculation. The eigenvalues obtained in this case are in excellent agreement with those values obtained by Ginsberg and Montroll, Hioe and Montroll, Pasupathy and Singh through their elaborated interpolation methods.

I. Introduction

Estimation of energy eigenstates of the quantum systems is one of the basic problems addressed by quantum mechanics. Such calculations are done by solving Schrodinger equation with specific potentials describing such systems. However, due to mathematical constraints, exact solutions are available only for a few types of potentials. Mention can be made of the harmonic oscillator, the coulomb, square well potentials etc. The quantum systems for which the potentials cannot be solved by Schrodinger equation are addressed by several approximation methods.

The harmonic oscillator is one of the fundamental systems in physics of vibrations and oscillations. It has gained vital importance in physics and other branches of science from both classical and quantum mechanical points of view ranging from crystal physics to black body radiation to elasticity to acoustics to lasers to molecular dynamics etc. In a simple harmonic oscillator, the motion of a particle of mass 'm' is constrained by a restoring force which is proportional to its displacement and acting towards its mean position. The potential energy of such a system is of the form $(x) = \frac{m\omega^2 x^2}{2}$, where ω is the angular frequency of the oscillator. Due to the nature of the potential, it is easy to mathematically examine the problem associated with harmonic oscillator. But, most of the physical oscillators are not exactly harmonic and the deviations from harmonic nature renders solution to Schrodinger equation inoperative in such physical systems. Such physical systems are referred to as 'Anharmonic oscillators'. In quantum anharmonic oscillators (AHO), in one dimension, the Hamiltonian takes the form

$$H = \frac{-\hbar^2}{2m}\frac{d^2}{dx^2} + \frac{1}{2}m\omega^2 x^2 + \lambda x^{2\alpha} \qquad (1)$$

The AHO Hamiltonian differs from that of harmonic oscillator by the potential term $x^{2\alpha}$, where $\alpha = 2,3,4, \ldots \ldots$, which corresponds to quartic, sextic, octic…. anharmonic oscillators. The coupling term $'\lambda'$ decides the anharmonicity of the system. $\lambda \neq 0, \omega = 0$ correspond to pure anharmonic oscillators. In the anharmonic term, the power of x is always even for bound states.

Quantum anharmonic oscillators have been extensively examined in literature by a variety of methods both from analytical and numerical points of view. Strong motivation for the study of AHOs is the result of the need for understanding vibrational spectra in the field of Molecular physics, Solid state physics, Quantum field theory etc. It is a well known fact that the vibrations of molecules, lattice vibrations in solid state materials are essentially anharmonic [1]. The AHO potential is also applied in nuclear structure, quantum chemistry and quark confinement studies [2], optical nonlinearities of conjugated polyenes [3]etc. Unfortunately, the AHO Hamiltonian cannot be solved by known exact mathematical methods. Among the wide range of approximate and numerical methods used for the study of AHOs, mention may be made of WKB method [4-5], Rayley Schrodinger perturbation method [6], action angle technique [7], Hill determinant method [8], continued fraction method [9], renormalized frequency [10], Chebyshev polynomial method [11], the residue squaring method [12], interpolative perturbation scheme [13], pade approximants method [14], differential method [15], kinetic potentials method [16], the fixed point method and the hepervirial method etc. The eigenvalues have been obtained to high orders of accuracy by numerical techniques and some authors have tried to obtain the functional dependence on the anharmonic co-efficient at the cost of numerical accuracy. In the present article, we have used variational method [17] that can be easily applied to several types of pure anharmonic oscillators. This is presented along with the best suited trial functions as suggested by Ginsberg and Montroll [18]. The results are further compared with those obtained from elaborate methods.

II. GROUND STATE WAVE FUNCTION FOR PURE QUANTUM ANHARMONIC OSCILLATORS

C.A Ginsberg and E.W. Montroll [18] have developed a method called "Interpolative perturbation scheme" for the determination of the eigenvalues and eigenfunctions of anharmonic oscillators. In this method a wave function with proper asymptotic behavior is chosen. The wave function is further constructed with other interpolative terms. The coefficients of the interpolative powers are determined by solving the Schrodinger equation near the origin. The coefficients lead to a polynomial equation for the energy eigenvalues that result from the requirements of self consistency. For pure quantum anharmonic oscillators the potential term can be written as

$$V(x) = \lambda x^{2\alpha} \qquad (2)$$

Where $\alpha = 2, 3, 4 \ldots \ldots \ldots$ are called quartic, sextic, octic .... oscillators respectively. Anharmonicity basically arises due to nonlinearity in the forces involved.

Thus the Schrodinger equation for pure anharmonic systems is written as

$$\left[\frac{-\hbar^2}{2m}\frac{d^2}{dx^2} + \lambda x^{2\alpha}\right]\psi(\mathrm{x}) = \mathrm{E}\psi(\mathrm{x})$$

Taking $\hbar = m = 1$, the Hamiltonian takes the form

$$\left[-\frac{d^2}{dx^2} + \lambda x^{2\alpha}\right]\psi(\mathrm{x}) = \mathrm{E}\psi(\mathrm{x}) \qquad (3)$$

The best suited trial functions as suggested by Ginsberg and Montroll [18] for ground state wave functions in the first approximation, for high anharmonicity constant can be written as follows:

For Quartic oscillator

$$\psi_0^{(4)}(x,\alpha) = Exp[-\alpha|x^3|] \quad (4)$$

For Sextic oscillator

$$\psi_0^{(6)}(x,\beta) = Exp[-\beta x^4] \quad (5)$$

For Octic oscillator

$$\psi_0^{(8)}(x,\delta) = Exp[-\delta|x^5|] \quad (6)$$

Where α, β and δ are the adjustable parameters, which we take them as variational parameters. These parameters determine the width of the wave function is shown below

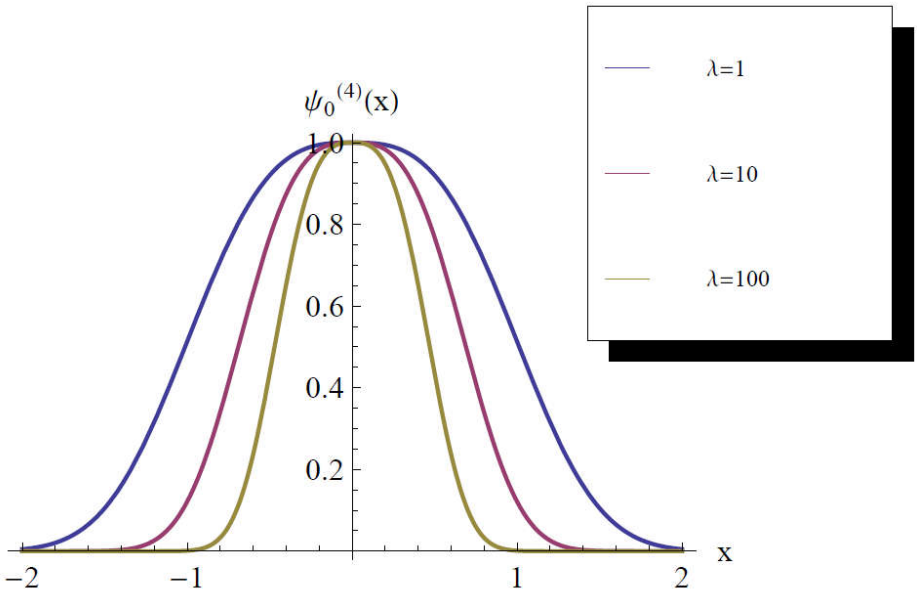

Figure 1: Plot of ground state wave function of a quartic oscillator for different anharmonicity constants

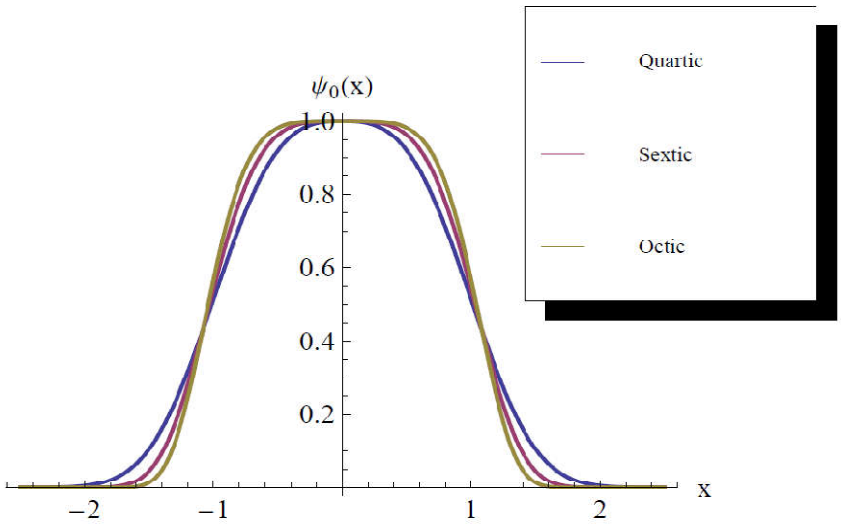

Figure 2: Plot of ground state wave functions of pure anharmonic oscillators for a fixed anharmonicity value

III. ESTIMATION OF GROUND STATE ENERGY OF A QUARTIC OSCILLATOR

For a quartic oscillator the potential term is written as $V(x) = \lambda x^4$. Keeping in mind all the features of ground state such as definite parity, zero nodes etc, we choose the trial function as

$$\psi_0^{(4)}(x,\alpha) = Exp[-\alpha|x^3|] \qquad (7)$$

Therefore the Hamiltonian for quartic oscillator is written as

$$H = -\frac{d^2}{dx^2} + \lambda x^4$$

Thus the expectation value of the Hamiltonian in the ground state wave function could be written as

$$E_0^{(4)}(\alpha) = \frac{\langle\psi(\alpha)|H|\psi(\alpha)\rangle}{\langle\psi(\alpha)|\psi(\alpha)\rangle} = \frac{\int_0^\infty \psi^{*(4)}_0(x,\alpha)\left[-\frac{d^2}{dx^2} + \lambda x^4\right]\psi_0^{(4)}(x,\alpha)\mathrm{dx}}{\int_0^\infty \psi^{*(4)}_0(x,\alpha)\psi_0^{(4)}(x,\alpha)\mathrm{dx}} \qquad (8)$$

The above equation, on simplification yields

$$E_0^{(4)}(\alpha) = \frac{0.60178\alpha^2 + 0.13373\lambda}{\alpha^{4/3}} \qquad (9)$$

Further, minimizing $E_0^{(4)}(\alpha)$ with respect to α, by taking $\frac{d}{d\alpha}\left(E_0^{(4)}(\alpha)\right) = 0$, we get

$$\alpha = 0.66667\sqrt{\lambda} \qquad (10)$$

Substituting the value of α in (9), we get an upper bound for the ground state energy of a pure quartic oscillator as

$$E_0^{(4)} \geq 0.68887\lambda^{1/3} \qquad (11)$$

This is in very good agreement with the values computed by Hioe and Montroll(1975) [19]; Pasupathy and Singh(1980)[20] , through elaborative interpolative methods, determined the ground state energy eigen values of a pure quartic oscillator as

$$E_0^{(4)} = 0.667986\lambda^{1/3}.$$

The plot of the eigen energies calculated by us is compared with those of Hioe and Montroll (1975); Pasupathy and Singh (1980) and are shown below

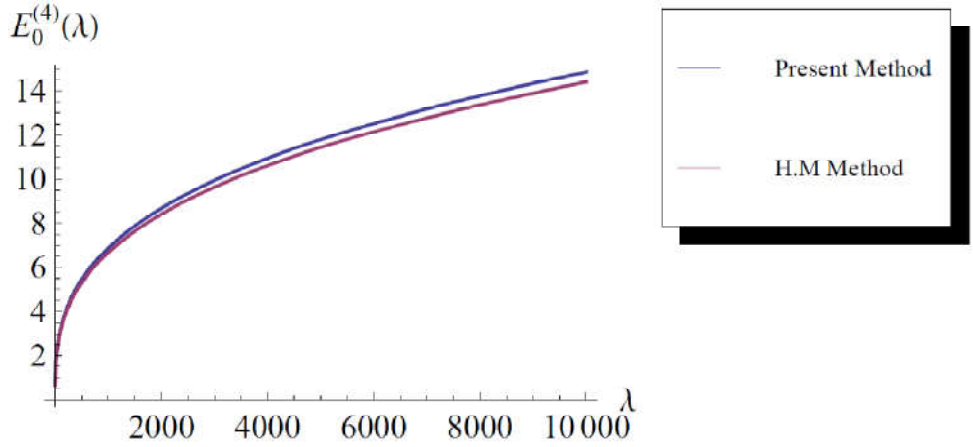

Figure 3: Comparison of ground state energies of quartic oscillator as calculated from the variational principle and Hioe- Montroll method

For some typical values of anharmonicity constant (λ) the ground state energy eigenvalues of a pure quartic oscillator are compared in the following table.

Table 1: Comparison of ground state energies of quartic oscillator as calculated from the variational principle and Hioe- Montroll method

λ	$E_0^{(4)}$ estimated from Rayleigh-Ritz variational method	$E_0^{(4)}$ estimated from Hioe-Montroll perturbative method
1.0	0.688872	0.667986
10.0	1.48413	1.43913
100.0	3.19746	3.10052
1000.0	6.88872	6.67986
10000.0	14.8413	14.3913

IV. ESTIMATION OF GROUND STATE ENERGY OF SEXTIC AND OCTIC OSCILLATOR

For a sextic and octic oscillators the potential term is written as $V(x) = \lambda x^6$ and $V(x) = \lambda x^8$ respectively. Considering the properties of wave functions at the ground state, we choose the trial functions as follows

For Sextic oscillator

$$\psi_0^{(6)}(x,\beta) = Exp[-\beta x^4] \quad (12)$$

For Octic oscillator

$$\psi_0^{(8)}(x,\delta) = Exp[-\delta|x^5|] \quad (13)$$

Thus the expectation value of the Hamiltonian in the ground state wave function for sextic oscillators could be respectively written as

$$E_0^{(6)}(\beta) = \frac{\langle\psi(\beta)|H|\psi(\beta)\rangle}{\langle\psi(\beta)|\psi(\beta)\rangle} = \frac{\int_0^\infty \psi^{*(6)}_0(x,\beta)\left[-\frac{d^2}{dx^2}+\lambda x^6\right]\psi_0^{(6)}(x,\beta)\mathrm{dx}}{\int_0^\infty \psi^{*(6)}_0(x,\beta)\psi_0^{(6)}(x,\beta)\mathrm{dx}} \quad (14)$$

And

$$E_0^{(8)}(\delta) = \frac{\langle\psi(\delta)|H|\psi(\delta)\rangle}{\langle\psi(\delta)|\psi(\delta)\rangle} = \frac{\int_0^\infty \psi^{*(8)}_0(x,\delta)\left[-\frac{d^2}{dx^2}+\lambda x^8\right]\psi_0^{(8)}(x,\delta)\mathrm{dx}}{\int_0^\infty \psi^{*(8)}_0(x,\delta)\psi_0^{(8)}(x,\delta)\mathrm{dx}} \quad (15)$$

Minimizing equation (14) and equation (15) with respect to the corresponding variational parameters β and δ, we get the upper bound for the ground state energy of a pure sextic oscillator as

$$E_0^{(6)} \geq 0.74809\lambda^{1/4} \quad (16)$$

and the corresponding upper bound for the ground state energy of a pure octic oscillator as

$$E_0^{(8)} \geq 0.832603\ \lambda^{1/5} \quad (17)$$

These are computed using Mathematica [21]. They are in very good agreement with the values computed by Ginsberg and Montroll through an elaborative interpolative method, which determines the ground state energy eigen values of a pure sextic oscillator as

$$E_0^{(6)} \geq 0.7194\lambda^{1/4} \quad (18)$$

And the corresponding ground state energy of a pure octic oscillator as

$$E_0^{(8)} \geq 0.7512\ \lambda^{1/5} \quad (19)$$

The plot of the eigen energies calculated by us is compared with those of Ginsberg et.al., and are shown below

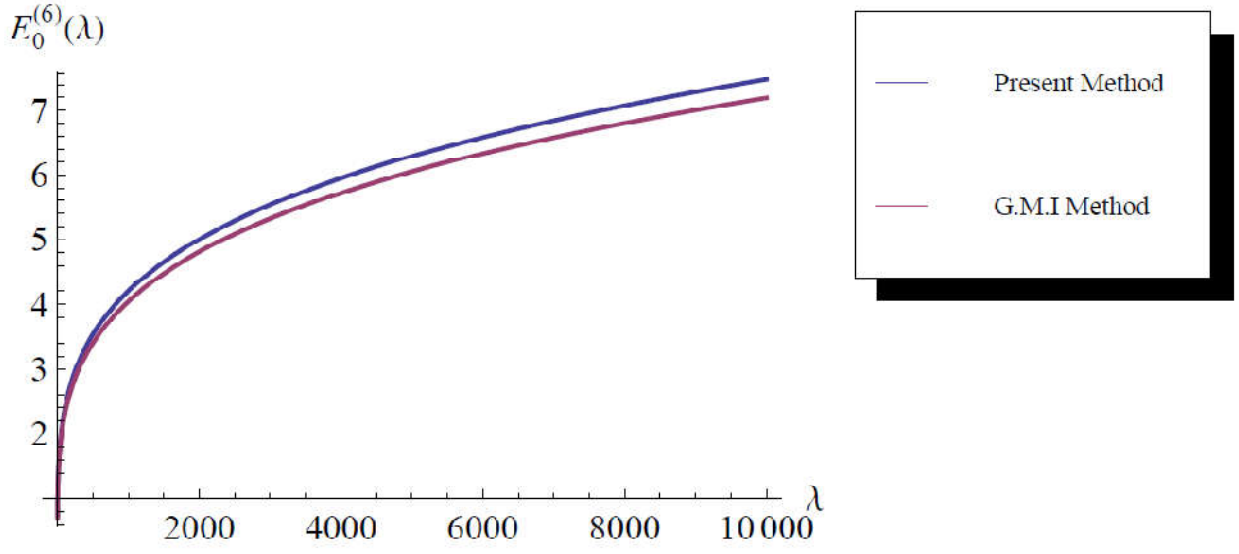

Figure 4: Comparison of ground state energies of sextic oscillator as calculated from the variation principle and Ginsberg- Montroll metho.

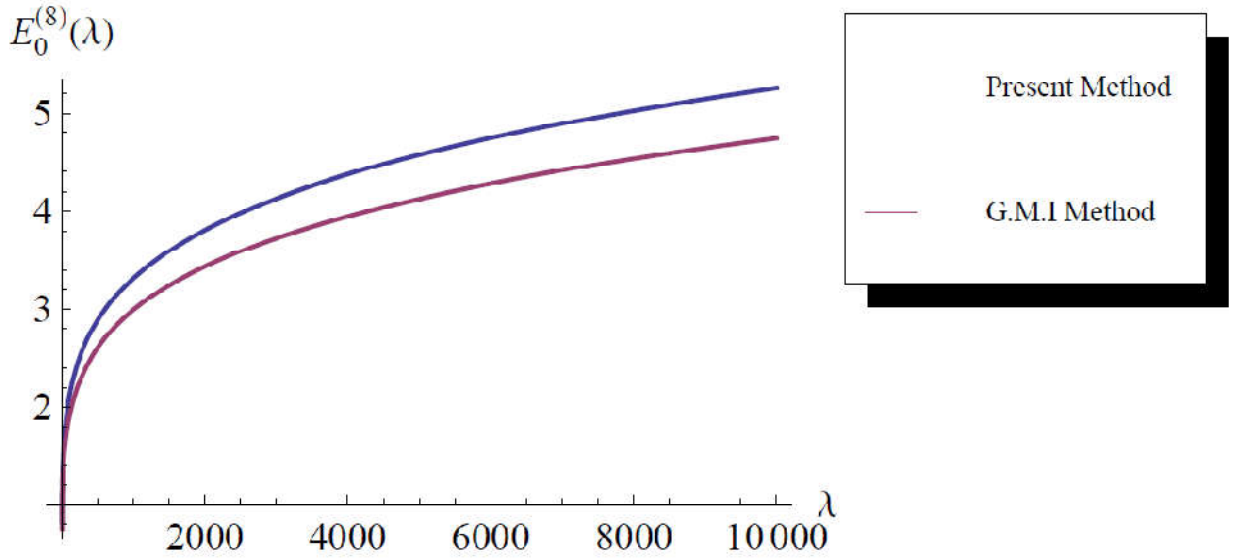

Figure 5: Comparison of ground state energies of octic oscillator as calculated from the variation principle and Ginsberg- Montroll Interpolation method

For few typical values of anharmonicity constant (λ) the ground state energy eigenvalues of a pure sextic and octic oscillators are compared in the following table.

Table 2: Comparison of ground state energies of Sextic and Octic oscillators as calculated from the variational principle and Ginsberg- Montroll method

λ	Sextic oscillator		Octic oscillator	
	$E_0^{(6)}$ estimated from Rayleigh-Ritz variational method	$E_0^{(6)}$ estimated from Ginsberg-Montroll perturbative method	$E_0^{(8)}$ estimated from Rayleigh-Ritz variational method	$E_0^{(8)}$ estimated from Ginsberg-Montroll perturbative method
1.0	0.748093	0.7194	0.832603	0.7512
10.0	1.33032	1.2792	1.31959	1.1905
100.0	2.36568	2.2749	2.09141	1.8870
1000.0	4.20684	4.0454	3.31465	2.9905
10000.0	7.48093	7.1940	5.25337	4.7397

V. RESULTS AND DISCUSSIONS

Quantum anharmonic oscillators play a significant role in understanding vibrations of crystal lattice, molecular vibrations in non-linear optical materials etc. Due to the form of the potential that is used to describe them, they cannot be solved exactly by analytical methods. The numerical and approximation methods used to examine quantum anharmonic oscillators are elaborate and mathematically specialized. Therefore in this article we have used a fairly simple method known as Rayleigh-Ritz variational method to calculate

the ground state energy eigenvalues of pure quantum anharmonic oscillators using appropriate asymptotic wave functions suggested by Ginsberg and Montroll. The eigenvalues calculated by us for three quantum anharmonic oscillators namely, quartic, sextic and octic oscillators are compared with the eigenvalues calculated for these systems by complex mathematical techniques. They are shown in figures 3 to 5 respectively. These graphs illustrate a good agreement between the values computed by us and the values obtained by Ginsberg and Montroll, Hioe and Montroll, Pasupathy and Singh through their elaborative interpolation methods. One distinct feature of the method which we have used is 'simplicity'. While other methods involved complex mathematics, the method which we have used is not so. Mathematics is simplified without compromising much on the accuracy of the result. Therefore it has considerable pedagogical value and it can be easily used to compute energy spectrum of anharmonic oscillators.

VI. ACKNOWLEDGEMENT

The authors thank Dr. B.A Kagali, former Professor of Physics, Bangalore University, Bengaluru and M.R Nandan, former Associate Professor of Philosophy, Government College for Women, Mandya, for their valuable suggestions for the improvement of this article. Authors are greatful to Principal and Head of department of Physics (Post Graduate), Government College (Autonomous), Mandya for facilitating the required research.

VII. REFERENCES

[1] Kittel, C., Introduction to solid state physics, 5th edition, Wiley Eastern Limited, Reprint (1992).

[2] Itzykson, C. and Zuber, J.B., *Quantum Field Theory*, Mc-Graw Hill,New York (1980).

[3] Daniel Loss and David P. Di Vincenzo, *Quantum computation with quantum dots*. Phys. Rev. A, 57(120), 1998.

[4] Tatsuya Koike. (1997). *Exact WKB analysis of Anharmonic Oscillators,* Kyoto University : Kyoto, Chapter-5

[5] M. Seetharaman, Sekhar Raghavan and S.S Vasan, *Analytic WKB energy expressions for three dimensional anharmonic oscillators*, J. Phys. A, **15(5),** pp 1537, (1982).

[6] Graffi, S. and Grccchi, V, *Rayleigh-Ritz Method, Secular determinant, and Anharmonic oscillators*, Phys. Rev. D, 8(10), pp 3487(1973).

[7] Gin-Yih Tsaur and Jyhpyng wang, Chinese J.Phys. **49(2),** pp555, (2011).

[8] S.N Biswas, K. Dutta, R.P Saxena, P.K Srivastava and V.S Varma, *Hill determinant:An application to the anharmonic oscillator*, Phys. Rev. D, **4(12)**, pp 3617, (1971).

[9] R.N Choudhuri, Phys. Rev. D, **31(10)**, pp2687, (1985).

[10] P.M Mathews, M. Seetharaman, Sekhar Raghavan and V.T. Bhargava, *A simple accurate formula for the energy levels of oscillators with a quartic potential*, Phys. Lett. **83A(3),** pp 118, (1981).

[11] J.P Boyd, J. Math. Phys., **19**, pp 1445, (1978).

[12] P.M Mathews, Pramana, **4**, pp 53, (1975).

[13] T. Shivalingaswamy and B.A Kagali, Ground States of Sextic and Octic Anharmonic Oscillators, Paripex-Indian Journal of Research, **3(7)**, pp 49, (2014).

[14] J. Leffel et.al., Phys. Lett. B, **30**, pp 656, (1969).

[15] Mouchet, A., A differential method for bounding ground state energy, J. Phys. A., 71(3). Pp247, 2005

[16] R. L Hall, Can.J. Phys. **63**, pp 311, (1985).

[17] W. N Mei, *Combined variational-perturbative approach to anharmonic oscillator problems,* Int. J. Math. Edu. Sci. Tech, **29(6)**, pp 875, (1998).

[18] C.A Ginsberg and E.W Montroll, *Application of a novel interpolative perturbation scheme to the determination of anharmonic wavefunctions,* J. Math. Phys., **19(1)**, pp 336, (1978).

[19] Hioe, F.T. and Montroll, E.W., *"Quantum theory of anhmmonic oscillators-Energy levels of oscillators with positive quartic anharmonicity",* J. of Math. Phys., 16(9), pp1945, (1975).

[20] Pasupathy,J. and Singh,V., University of Texas (Austin) preprint DOE -ER – 03992, pp 423 (1 980).

[21] Stephen Wolfram, *The Mathematica Book and Software*, (Cambridge:Cambridge University Press), (1996).

Error analysis in undergraduate Physics Lab

Surajit Sen[1]

[1]Department of Physics
Guru Charan College
Silchar 788004, India.
Email: ssen55@yahoo.com

(Submitted: 07-04-2017)

Abstract

The '*Error analysis*' is one of the most important corner stone of the experimental physics which should be given proper attention at the undergraduate (UG) level. In most of the UG Physics (Hons) laboratories, the calculation of error is often ended up with the calculation of '*Percentage Error*' without giving attention to the '*Standard Error*', which forms the basis of accepting or rejecting the experimental data. In this article we have discussed the methodology of calculating the *Standard Error* for common UG experiments in a pedagogical way.

1 Introduction

Experiments of an UG Physics Lab can be classified into following broad categories: a) Mechanics, b) Properties of Matter, c) Electricity and Magnetism, d) Optics, e) Waves and Oscillation, f) Heat and Thermodynamics, g) Electronics, h) Modern Physics and others. No matter whatever be the procedure, the *Error Analysis* is an integral part of every experiment to testify the acceptability of the experimental result. Although most physics practical books of Indian Universities give a detailed description of various experiments, but they do not give adequate space to illustrate the error analysis [1, 2, 3]. The pitfall is that, the importance of checking the reliability of experimental data is often overlooked both by the teachers as well as by the students. To fill up that gap, in this work

we have given an introduction of the elementary error analysis with special emphasize on the calculation of *Standard Error*. In a given experiment, it is important to know that, on measurement, which of the component of the device is contributing maximum error. The calculation of the *Standard Error*, which is indeed a measure of the error propagation, precisely addresses this issue and helps to fix that particular part of the experiment accordingly. In this paper, we have compiled the working formula of some UG experiments commonly used by the freshmen in their lab, and show that how to calculate the *Standard Error* from them.

The remaining Sections of the paper are organised as follows: In Section-I we have given an introduction of the statistical tools required for the error analysis. Section-II discusses we discuss the methodology of calculating the *Standard Error* for some specific UG physics experiments. Finally, we summarize our results in the Conclusion Section.

2 Statistical Analysis of Error

In science, '*Theory*' and '*Experiment*' are inseparable. In a physics lab, each experiment requires the purported measurement of a set of parameters (e.g., M, L, T, C etc.) by one or multiple number of devices which leads the accumulation of large amount of data. There exists two ways to bridge an 'Experiment' with the 'Theory' to draw correct inference:

a) A 'Theoretical Physicist' *predicts* a phenomenon by mathematical modelling and an 'Experimental Physicist' *verifies* that in the lab (or elsewhere) by so-called 'Experimental Observation'.

b) An 'Experimental Physicist' observes some phenomenon in the lab (or elsewhere) which a 'Theoretical Physicist' has to explain by the 'Mathematical Modelling'.

We note that in both of these routes, the generation of large amount of data becomes unavoidable. Under such circumstances, it is very important to note the difference between the observational result with the theoretical prediction subtracting out the error component by appropriate statistical analysis with an utmost care. In the history of physics, careful analysis of this difference often leads to the discovery of some 'New Physics', e.g., Perihelion shift in General Theory of Relativity, fine-structure constant in Quantum Electrodynamics etc.

2.1 Classification of error:

To extract the 'creamy' part, called 'experimental result', from large amount of data, we have to analyse it using basic laws of statistics. Before enunciating that, let us note the broad classification of error:

Systemic Error: The error which arises due to presence of some defect of an instrument is called *Systemic Error*. For example, a slide calipers is often found to have an instrumental error which is an example of Systematic Error.

Random Error: The repetitive measurement leads to the generation of data which never coincide with each other.

Such error is called *Random Error* which is due to fluctuation of temperature/pressure/current/voltage and even due to the vibration of working table or the change of local ambience.

Personal Error: The error, which is induced due to the careless collection (or mistake) of the experimental data, is called *Personal Error*.

The *Systematic Error* can be fixed by improving the experimental device, while the *Random Error*, in general, has to be analysed statistically. The key difference between these two kind of errors is conventionally illustrated by the Fig.[1] and Fig.[2], respectively [4].

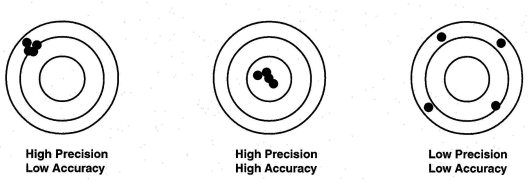

Figure 1: 'Random Error' implies 'Precision', while 'Systemic Error' implies 'Accuracy'

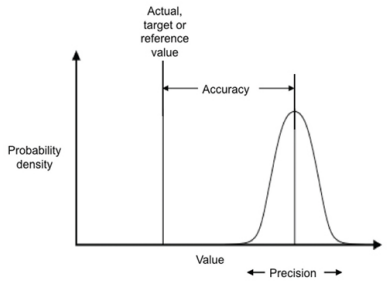

Figure 2: Comparison of 'Random' and 'Systemic' Error

The *Percentage Error* is used to measure the difference of the experimental value from the theoretical one, while the *Standard Error* gives the statistical estimate of the departure from the accurate or theoretical value. To understand the error of this kind, which is missing from most of our physics practical books, we have to understand *Error Propagation*.

Error propagation: The working formula of a given experiment is a function of some parameters which have to be measured repeatedly. For example, to find the acceleration due to gravity, we need to measure the value of the time period (T) and length (L) of the pendulum, i.e., $g = g(T, L)$. The value of successive measurements of these parameters never coincide and in consequence, the error is induced. Thus it is inevitable that, the error in the measurement of T or L is 'propagated' in the determination of the value of g. Such character of error is often referred as *Error Propagation* which has to be analysed statistically. The error or uncertainty induced due to that is called *Standard Error* (S.E.) and in the following section we discuss its brief derivation [5, 6].

2.2 Calculation of Standard Error

In an experiment, we often need to calculate the error associated with an unknown function $f(x_i)$ by N number of repetitive measurement of known parameters x_i, which is referred as 'data'. Then the error in the measurement of a function $f(x_i)$ is a cumulative effect of the error in the individual measurement of the parameter x_i $(i = 1, 2, \ldots N)$. To

calculate the S.E., which is indeed the '*Standard Deviation of the Mean*', we follow the following steps:

Using the principle of least square method, the fractional uncertainty of the function $f(x_i)$ is given by,

$$\frac{\delta f}{f} = \sqrt{\left(\frac{1}{f}\frac{\partial f}{\partial x_1}\right)^2 \delta x_1^2 + \left(\frac{1}{f}\frac{\partial f}{\partial x_2}\right)^2 \delta x_2^2 + \cdots + \left(\frac{1}{f}\frac{\partial f}{\partial x_N}\right)^2 \delta x_N^2}. \quad (1)$$

Then for a given function $f(x_i)$, the S.E. of a set of data is defined as,

$$\Delta f = \bar{f}\sqrt{\left(\frac{\Delta x_1}{\overline{Q}_1}\right)^2 + \left(\frac{\Delta x_i}{\overline{Q}_2}\right)^2 + \cdots + \left(\frac{\Delta x_N}{\overline{Q}_N}\right)^2}, \quad (2)$$

where $\bar{f}$ be the '*Mean Value*' of the function $f(x_i)$ and $\overline{Q_i}(x_1, x_2, \ldots x_N)$ be the mean of the polynomial of x_i. In Eq.(2) the S.E. corresponding to the measurement of the each parameter x_i is given by,

$$\Delta x_i = \frac{\sigma_{N-1}}{\sqrt{N}}, \quad (3)$$

where the *Standard Deviation* (σ_{N-1}) defined as,

$$\sigma_{N-1} = \sqrt{\frac{1}{N-1}\sum_{i=1}^{N}(x_i - \bar{x})^2}. \quad (4)$$

Thus the experimental value of the function with the error correction is given by

$$\boxed{f_{expt} = \bar{f} \pm \Delta f}. \quad (5)$$

It is customary to express the S.E. as the percentage of the mean value, i.e., $\frac{\Delta f}{f} \times 100\%$. In a typical UG lab, if the S.E. is less than 10% of the mean value, then the experimental result may be accepted. This requirement, however, varies from lab to lab depending upon local demand for higher precision. The mean value and the S.E. must be rounded up to same order of decimal. For example, the acceleration due to gravity with should be written as,

$$\boxed{g_{expt} = (978.89 \pm 11.56)/s^2}, \quad (6)$$

instead of $g_{expt} = (978.89 \pm 11.561)/s^2$. Here the S.E. is 1.18% of the mean value and therefore the result of the experiment is acceptable.

3 Standard Error of common UG experiments

In this section we have listed the formula necessary to calculate the S.E. of some common UG Physics experiments [7]. We have illustrated its calculation for the 'Bar Pendulum Experiment' in detail, while the treatment for remaining experiments is similar. For the derivation of the working formula and the meaning of the various symbols appearing in it, we refer the readers to consult any UG physics practical book, e.g., [1, 2].

i) **To determine the acceleration due to gravity by Bar Pendulum**

The working formula to calculate the acceleration due to gravity using bar pendulum is given by [2],

$$g = \frac{4\pi^2 L}{T^2} \equiv g(L,T), \tag{7}$$

where $L = l_1 + l_2$ be the equivalent length. From this formula, the uncertainty in calculating the acceleration due to gravity can be obtained,

$$\delta g = \sqrt{\left(\frac{\partial g}{\partial L}\right)^2 (\delta L)^2 + \left(\frac{\partial g}{\partial T}\right)^2 (\delta T)^2}. \tag{8}$$

Using Eq.(7), corresponding fractional uncertainty is given by,

$$\frac{\delta g}{g} = \sqrt{\left(\frac{\delta L}{L}\right)^2 + 4\left(\frac{\delta T}{T}\right)^2}. \tag{9}$$

Then the Standard Error in measuring the acceleration due to gravity is given by,

$$\Delta g = \bar{g}\sqrt{\left(\frac{\Delta L}{\bar{L}}\right)^2 + 4\left(\frac{\Delta T}{\bar{T}}\right)^2}, \tag{10}$$

where $\bar{g}$, $\bar{L}$ and $\bar{T}$ be their respective mean values calculated from the experiment. Comparing Eq.(10) with Eq.(2), we find $Q_1(L) = L$ and $Q_2(T) = T$, respectively. In Eq.(10), the S.E. in the determination of the equivalent length and time period are given by,

$$\Delta L = \sqrt{\frac{1}{N(N-1)} \sum_{i=1}^{N} (L_i - \bar{L})^2}, \tag{11}$$

$$\Delta T = \sqrt{\frac{1}{N(N-1)} \sum_{i=1}^{N} (T_i - \bar{T})^2}. \tag{12}$$

ii) **To determine the refractive index of water by travelling microscope**

The working formula to calculate the refractive index of liquid is given by [2],

$$\mu = \frac{R_3 - R_1}{R_3 - R_1} \equiv \mu(R_3, R_2, R_1), \tag{13}$$

and the S.E is calculated from the formula,

$$\Delta\mu = \bar{\mu}\sqrt{\left(\frac{\Delta R_1}{R_3 - R_1}\right)^2 + \left(\frac{\Delta R_2}{R_3 - R_2}\right)^2 + \left(\frac{\Delta R_3}{\frac{(R_3-R_1)(R_3-R_2)}{(R_2-R_1)}}\right)^2}, \quad (14)$$

Comparing Eq.(14) with Eq.(2), we find $Q_1(R_1, R_3) = R_3 - R_1$, $Q_2(R_2, R_3) = R_3 - R_2$ and $Q_3(R_1, R_2, R_3) = \frac{(R_3-R_1)(R_2-R_1)}{(R_2-R_1)}$, respectively.

iii) **To determine the Young's modulus of the material of the given wire by Searle apparatus**

The working formula of calculating the Young's modulus is given by,

$$Y = \frac{4MgL}{\pi d^2 l} \equiv Y(M, g, L, d, l). \quad (15)$$

Then the S.E. in calculating Young Modulus is given by,

$$\Delta Y = \bar{Y}\sqrt{\left(\frac{\Delta M}{\bar{M}}\right)^2 + \left(\frac{\Delta g}{\bar{g}}\right)^2 + 4\left(\frac{\Delta d}{\bar{d}}\right)^2 + \left(\frac{\Delta L}{\bar{L}}\right)^2 + \left(\frac{\Delta l}{\bar{l}}\right)^2}, \quad (16)$$

where the S.E. in the measurement of $x_i(M, g, L, d, l)$ are given by,

$$\Delta x_i = \sqrt{\frac{1}{N(N-1)}\sum_{i=1}^{N}(x_i - \bar{x})^2}. \quad (17)$$

iv) **To determine the rigidity modulus by statical method using Barton apparatus**

The working formula of calculating the rigidity modulus using torsional pendulum reads,

$$\eta = \frac{360^\circ MglD}{\pi^2 r^4 \phi} \equiv \eta(M, g, \phi, D, r, l), \quad (18)$$

where the symbols have their usual meaning [2]. The S.E is calculated from the formula,

$$\Delta\eta = \bar{\eta}\sqrt{\left(\frac{\Delta M}{\bar{M}}\right)^2 + \left(\frac{\Delta g}{\bar{g}}\right)^2 + \left(\frac{\Delta \phi}{\bar{\phi}}\right)^2 + \left(\frac{\Delta D}{\bar{D}}\right)^2 + 16\left(\frac{\Delta r}{\bar{r}}\right)^2 + \left(\frac{\Delta l}{\bar{l}}\right)^2}. \quad (19)$$

v) **To find the M.I. of unknown body by Torsional pendulum**

The working formula to calculate the Moment of Inertia is given by [2],

$$I_x = \frac{(L^2+b^2)}{12}\frac{T_x^2 - T_0^2}{T_1^2 - T_0^2} \equiv I_x(L, b, T_0, T_1, T_x), \tag{20}$$

and the formula for calculating the S.E. is given by,

$$\Delta I_x = 2\bar{I}_x \sqrt{\left(\frac{\Delta L}{\frac{L^2+b^2}{L}}\right)^2 + \left(\frac{\Delta b}{\frac{L^2+b^2}{b}}\right)^2 + \left(\frac{\Delta T_0}{\frac{(T_1^2-T_0^2)(T_x^2-T_0^2)}{T_0(T_1^2-T_x^2)}}\right)^2 + \left(\frac{\Delta T_1}{\frac{T_1^2-T_0^2}{T_1}}\right)^2 + \left(\frac{\Delta T_x}{\frac{T_x^2-T_0^2}{T_x}}\right)^2}. \tag{21}$$

vi) **To determine the of focal length of the given concave lens with the help of auxiliary convex lens**

The working formula to calculate the focal length is given by [2],

$$f = \frac{UV}{U-V} \equiv \mu(U, V), \tag{22}$$

and the S.E is calculated from the formula,

$$\Delta f = \bar{f}\sqrt{\left(\frac{\Delta U}{\frac{U(U-V)}{V}}\right)^2 + \left(\frac{\Delta V}{\frac{V(U-V)}{U}}\right)^2}. \tag{23}$$

vii) **To determine the refractive index of water by a convex lens and plane mirror**

The working formula to calculate the refractive index of liquid is given by [2],

$$\mu = 1 + \frac{R}{f_2} \equiv \mu(R, f_2), \tag{24}$$

and the S.E is calculated from the formula,

$$\Delta\mu = \bar{\mu}\sqrt{\left(\frac{\Delta R}{R+f_2}\right)^2 + \left(\frac{\Delta f_2}{f_2(1+\frac{f_2}{R})}\right)^2}. \tag{25}$$

viii) **To determine the specific resistance of the materials of a given wire by metre-bridge**

The working formula to calculate the specific resistance of the material of the

meter bridge wire is given by [2],

$$\rho = \frac{\pi d^2 R}{4L} \equiv \rho(d, R, L), \qquad (26)$$

and the formula for calculating the S.E. is given by,

$$\Delta\rho = \bar{\rho}\sqrt{4\left(\frac{\Delta d}{\bar{d}}\right)^2 + \left(\frac{\Delta R}{\bar{R}}\right)^2 + \left(\frac{\Delta L}{\bar{L}}\right)^2}. \qquad (27)$$

ix) **To determine the resistance per unit length of a metre-bridge wire by Carey-Foster method**

The working formula to calculate the specific resistance of the material of the meter bridge wire is given by [2],

$$\rho = \frac{X}{l_1 - l_2} \equiv \rho(X, l_1, l_2), \qquad (28)$$

and the formula for calculating the S.E. is given by,

$$\Delta\rho = \bar{\rho}\sqrt{\left(\frac{\Delta X}{\overline{X}}\right)^2 + \left(\frac{\Delta l_1}{\overline{l_1 - l_2}}\right)^2 + \left(\frac{\Delta l_2}{\overline{l_1 - l_2}}\right)^2}. \qquad (29)$$

x) **To determine the value of the given low resistance by drop of potential method using metre-bridge**

The working formula to calculate the specific resistance of the material of the meter bridge wire is given by [2],

$$X = R\frac{l_2}{l_1} \equiv \rho(R, l_1, l_2), \qquad (30)$$

and the formula for calculating the S.E. is given by,

$$\Delta X = \bar{X}\sqrt{\left(\frac{\Delta R}{\overline{R}}\right)^2 + \left(\frac{\Delta l_1}{\overline{l_1}}\right)^2 + \left(\frac{\Delta l_2}{\overline{l_2}}\right)^2}. \qquad (31)$$

xi) **To determine the internal resistance by potentiometer**

The working formula to calculate the internal resistance of the material of the meter bridge wire is given by [2],

$$r = R\frac{l_1 - l_2}{l_2} \equiv r(R, l_1, l_2), \qquad (32)$$

and the formula for calculating the S.E. is given by,

$$\Delta r = \bar{r}\sqrt{\left(\frac{\Delta R}{\bar{R}}\right)^2 + \left(\frac{\Delta l_1}{\overline{l_1 - l_2}}\right)^2 + \left(\frac{\Delta l_2}{\overline{l_2}}\right)^2}. \qquad (33)$$

xii) **To compare of low resistance by potentiometer**

The working formula for comparing two low resistances ($x = \frac{X}{R}$) using potentiometer [2] given by,

$$x = \frac{l_1}{l_2} \equiv x(l_1, l_2), \tag{34}$$

and the formula for calculating the S.E. is given by,

$$\Delta x = \bar{x}\sqrt{\left(\frac{\Delta l_1}{\overline{l_1}}\right)^2 + \left(\frac{\Delta l_2}{\overline{l_2}}\right)^2}. \tag{35}$$

xiii) **To determine the reduction factor of tangent galvanometer**

The working formula to calculate the reduction factor of tangent galvanometer [2],

$$K = \frac{W}{10Zt\tan\theta} \equiv K(W, Z, t, \theta), \tag{36}$$

and the formula for calculating the S.E. is given by,

$$\Delta K = \bar{K}\sqrt{\left(\frac{\Delta W}{\overline{W}}\right)^2 + \left(\frac{\Delta Z}{\overline{Z}}\right)^2 + \left(\frac{\Delta t}{\bar{t}}\right)^2 + 4\left(\frac{\Delta\theta}{\overline{\sin 2\theta}}\right)^2}. \tag{37}$$

4 Conclusion

In this article we have discussed the tenet of the error analysis in a pedagogical way. We hope such step-by-step approach will give the students a hands-on experience to calculate the *Standard Error* with the modest amount of data they collect in their UG lab and revise the 'Error Analysis' section of their laboratory notebook accordingly. Our experience is that, the pragmatic method outlined above has a very special appeal to the Physics (Hons) freshmen, who can easily extend it for the advanced experiments in their sophomore and final years.

Acknowledgments

I thank Dr M R Nath and Dr T K Dey for their suggestion. I owe the Physics (Hons) students of our college, who, through their repeated queries, help me to prepare it in a pedagogical way.

References

[1] Chattopadhyay, D., Rakshit, P. C. and Saha, B., *An Advanced Course in Practical Physics*, New Central Book Agency, Kolkata (2005)

[2] Ghosh, S. K., *An Advanced Course in Practical Physics*, New Central Book

Agency, Kolkata (2012)

[3] Flint B. L., Worsnop, H. T., *Advanced Practical Physics for Students*, Asia Publishing House (P) Ltd, New Delhi (1963)

[4] See, for example, Wilson, J.D., Hernndez-Hall, C. A. , *Physics Laboratory Experiments*, Brooks/Cole, Cengage Learning, Boston (2010)

[5] Taylor J. R., *Introduction to Error Analysis: The study of uncertainties in Physical Measurements*, Science Books, Sauselito, CA (1997)

[6] Baird, D.C., Experimentation: An Introduction to Measurement Theory and Experiment Design, 3rd. ed. Prentice Hall: Englewood Cliffs, (1995)

[7] Sen, S., Talk given at NIT, Aizwl (2013) Error calculation in UG Physics Lab

Gender Gap and Polarisation of Physics on Global Courses

A. L. Alinea[1] and W. Naylor[2]

[1]Department of Physics, Osaka University
Toyonaka City, Osaka Prefecture 560-0043, Japan.
allanlalinea@gmail.com

[2]Redcliffe State High School
Queensland, Australia.
wxnay0@eq.edu.au

(Submitted 20-02-2017)

Abstract

We examine the gender aspect of 'polarisation' in connection with student response to the six polarisation-inducing questions in the Force Concept Inventory (FCI). The test (pre and post) was given to first year classical mechanics students ($N = 66$ students, over four years) enrolled in an international (global) course at Osaka University, Japan. Our data suggest that the 'polarisation' phenomenon is not unique to one gender. Furthermore, the extent by which it is exhibited by males may differ from that of females at the beginning (pretest) but the gap closes upon learning more about forces (posttest). These findings are for the most part, complemented by our result for the FCI as a whole. Although the differences in means for males and females may suggest a gender gap, statistical analysis shows that there is no gender difference at the 95% confidence level.

1 Introduction

It can be said that the Newton's laws of motion, the three pillars of Newtonian mechanics, are all about force. This is the reason why in a class on (elementary) Newtonian mechanics, much of the quantitative and conceptual problems that students are expected to solve involve friction, gravity, tension, weight, etc., in connection with elevators, pendula, bridges, projectiles, and other physical systems. In all of these problems, when it comes to dynamics, everyone essentially starts with the basics of the Free Body Diagram (FBD). And when it comes to FBDs, everybody begins with identifying forces: 'What are the forces acting on a given body?' This is very basic. Yet the basic skill of identifying forces propagates up to the pinnacle of complexity involved in building bridges and towers, constructing satellites, and creating machinery in factories, amongst others. In the Force Concept Inventory [1, 2, 3] regarded as the *de facto* standard for concept inventories in Newtonian mechanics, six (that is, 20%) of the 30 questions basically ask only one thing: identify the forces acting on a given body. This demonstrates the importance of learning this basic skill cannot be overemphasized.

In our previous work [4], we focused on these six FCI questions[1] and investigated how our students on global courses at Osaka University, Japan [5] answered them. Surprisingly, we found a 'phenomenon' called *polarisation*. To wit, given five choices corresponding to five sets of forces acting on a body specified in an FCI question, the great majority of students elected only two letters—the *polarising choices*—out of five choices (see Fig. 1). This pair of choices consists of two sets of forces with one being a subset of the other. The subset in the pair is the correct answer while the other one includes an extra 'fictitious' force not legitimately acting on the body. Students who are otherwise knowledgeable about the acting forces are confused with the addition of the wrong force; thus, resulting to polarisation. We explained that such a 'phenomenon' may be attributed to *misleading ontological categorisation* [6]. In the concluding remarks, as part of our future prospect, we opened the door to further investigation of this matter—causes, cure, and other aspects of polarisation.

In the current paper, focusing on the possible *gender aspect* of polarisation, we investigate *gender gap* [7, 8, 9, 10, 11]. Gender gap is the resulting gender difference (in favour of males) in the student performance on standardised assessments such as the FCI. Such a delicate concept has so far found no simple explanation and complete 'cure' that are supported by repeatable experiments. We are not here going to pretend to fill in the absence of a complete explanation and 'cure'. Our aim is more modest and being such, should be answerable at least within the range of validity of the available data that we have. We want to know if there is a gender aspect associated with polarisation. To this end, we wish (a) to determine whether polarisation is unique to one gender, and if it is not, (b) to establish if there is a gender difference asso-

[1] These are the sets of questions {5, 11, 13, 18, 29, 30} in the FCI.

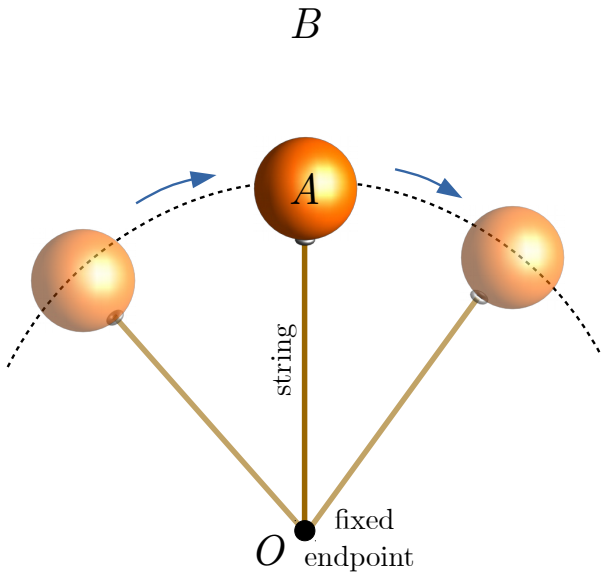

i. tensional force from A to O
ii. downward force of gravity
iii. upward force from A to B

Five Choices:

A.) i only

B.) ii only

C.) iii only

D.) i and ii only ✓

E.) i, ii, and iii ✗

polarising choices

Figure 1: A student may be asked to identify the forces acting on an object undergoing a vertical circular motion when the object is at its highest point, with the following set of forces given by (i), (ii), and (iii) above. The five choices are indicated by the letters A to E above. Whereas most students with average preparation may be able to identify (i) and (ii) as the correct set of forces, the addition of (iii) may confuse them. This can lead to polarisation where most students may choose (D) or (E). (Note: This example is for illustrative purposes only and has not been tested if it would induce polarisation. We used only FCI questions in our study.)

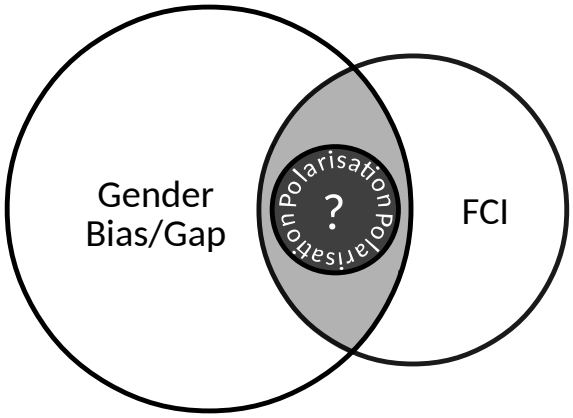

Figure 2: Venn diagram for polarisation, gender bias/gap, and the FCI.

ciated with the extent by which polarisation is exhibited by students. As far as we know, this study is a first of its kind to examine the possible gender dimension of polarisation. It has the added value that the subjects of our study are mostly international students (see Sec. 2).

Graphically, the mentioned objectives can be represented in a unified way through the placement of the circle for polarisation in the Venn diagram shown in Fig. 2. Considering that the gender gap/bias extends beyond the FCI (eg., in other concept inventories, gender bias on Wikipedia [12], etc), we have drawn a bigger circle for it and made it partially intersect with the circle for the FCI. Such a partial intersection is justified, noting that only partial gender gap/bias may exist. With the six polarisation-inducing questions within the FCI, we want to know where the corresponding circle for polarisation should be placed. Depending on our result, it may be completely moved out of the light gray-shaded region, meaning no gender gap, or it may be pushed a little further from its current location, partially intersecting with the big circle for gender gap/bias.

2 Methodology

The subjects of our testing are the students of the Chemistry-Biology Combined Major Program (CBCMP). This is a four-year program offered by Osaka University (Japan), open to all qualified students from all over the globe. Approximately 90% of our students came from outside Japan. With English as the medium of instruction, all applicants are required to have sufficient English ability to be accepted. Considering all entrants, the average equivalent TOEFL score[2] is 104 with a standard deviation of 14. Such a high average with relatively low standard deviation suggests that English ability is not a factor that could significantly affect performance on the FCI; this, we found out in our previous work [4].

In total, starting from AY 2011-12, we have 66 students (56% females and 44% males) corresponding to four batches of entrants. These students attended a calculus-based introductory Newtonian mechanics class under our supervision. Each class meeting lasts for 1.5 hours (90 minutes) and is conducted once a week for a period of four months.[3]

[2]We performed the necessary conversion for some students who took IELTS. Furthermore, we assigned full score for native speakers.

[3]This relatively tight schedule is a common setting

A typical class starts with a discussion of pre-lecture conceptual questions as refresher. These questions are usually given as assignment one meeting before the class to prepare the students. A short lecture then follows highlighting the main points of the subject for the day. After this, for the remaining 50 minutes, students are paired[4] to answer questions on MasteringPhysics™ [16]. While solving conceptual and quantitative problems, the teaching assistant and the instructor go around the room to attend to student concerns about the problem they are solving. The students are given one week to finish the assigned task.

We administered the FCI at the beginning and end of every second semester from AY 2011-12 to AY 2014-15. All student answers were recorded and an item analysis was performed with emphasis on the six polarisation-inducing questions. Standard statistical parameters for the four-year data were calculated including p-value for t-test and chi-squared test,[5] mean, standard deviation, percent difference, etc., through R [19] and a spreadsheet. Using these parameters, (a) student performance from pretest to posttest, (b) possible gender difference in overall FCI, (c) existence of polarisation, (d) possible gender difference in the polarisation-inducing questions, among others, were analysed.

for university lecture classes in Japan.

[4]See refs. [13], [14], and [15], and the references therein for the benefits of peer discussion/instruction.

[5]Interested readers who wish to familiarise themselves with the basics of statistical analysis including t-test, chi-squared test, and measures of variation (eg., standard deviation and standard error of the mean), among others, may want to consult refs. [17] and [18].

3 Polarisation

3.1 Polarisation as a Whole

Before we delve into the issue of the possible gender aspect of polarisation, we look at the extent of this phenomenon for all students irrespective of gender. Figure 3 shows the pair of dominant answers for questions I to VI. This pair as we pointed out in our previous work [4] is composed of a correct choice (CC) and a wrong choice (X), where CC happens to be a subset of X; eg., in question I, these are choices (CC, X) = (B,D). Here, with our updated data,[6] we once again confirm the observation that majority of students only select two choices. For the pretest at least 61% with a maximum of 86% elected the polarising choices. It rose to at least 76% in the posttest with an astonishing maximum of 95%.

Figure 4 shows a vivid graphical display of such polarisation from pretest to posttest. As can be seen in the figure, overall, there is a general increase in the proportion of students who elected the polarising choices from pretest to posttest. In tandem with Fig. 3, we see that such a trend is strictly followed for all questions for the choice CC, and mod-

[6]We have to re-confirm polarisation with our updated dataset to set the ground for examining its possible gender aspect. Needless to say, we cannot examine the possible gender gap associated with a phenomenon that we cannot ascertain.

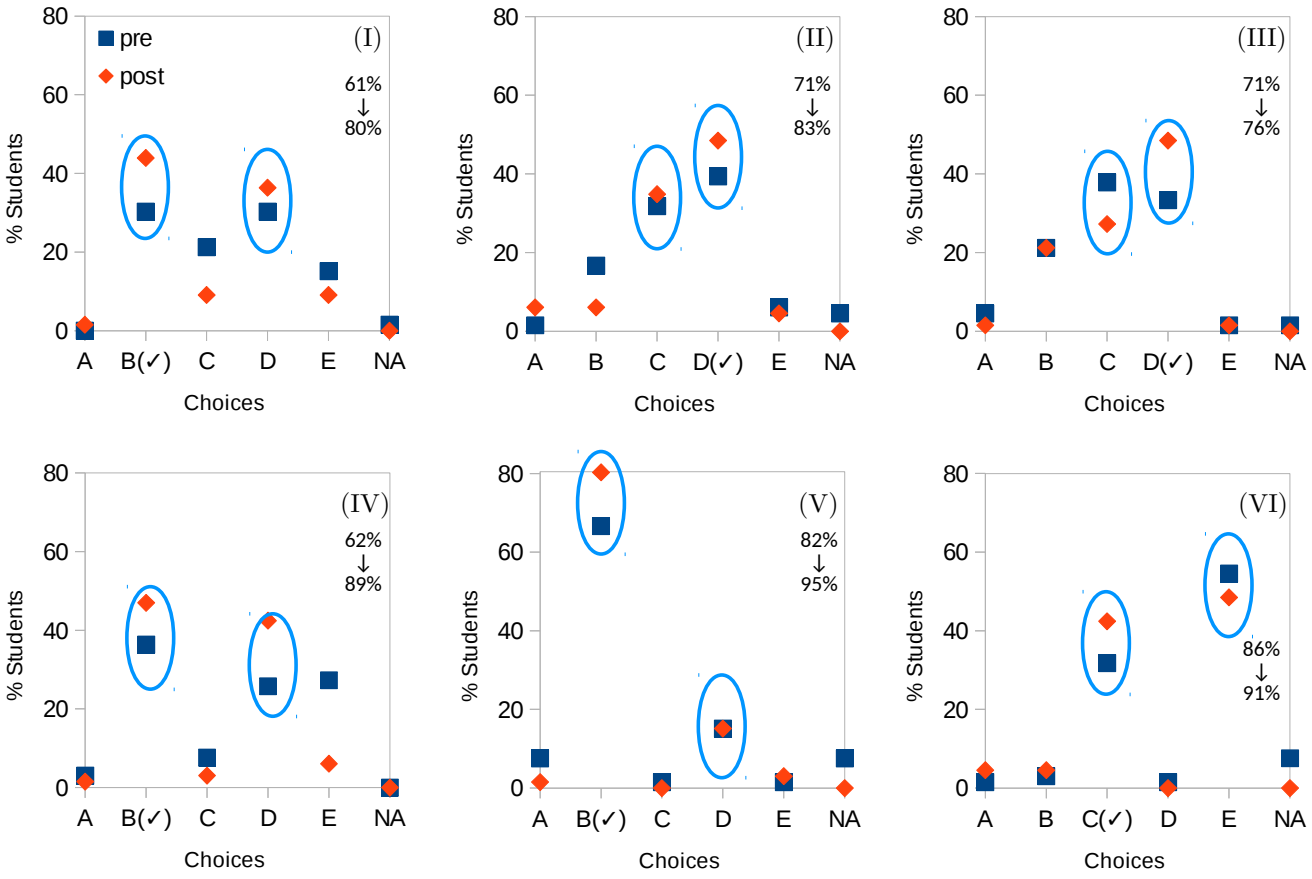

Figure 3: Distribution of student answers for questions I to VI. The set of five choices spans from letters A to E, with NA corresponding to no answer. The correct answer for each question is labelled with a check mark. For each question, two letters (including the correct answer) take the majority share of student answers (see the encircled data points). The two numbers at the right part of each graph indicate the percent of students who chose these so-called *polarising choices* from pretest to posttest.

erately obeyed for the choice X (see graphs for questions III and VI). A detailed examination of student responses indicates that the increase in the share for CC has a major contribution due to the migration of students who elected X in the pretest to CC in the posttest; that is, from being 'confused' to 'enlightened'. More specifically, of all the transitions from the four wrong choices to CC, 54% came from X → CC. Students who were once confused by the 'fictitious' force in X, learned along the way, and elected CC in the posttest. This however, did not in general, decreased the share for X. Some students who elected the *other* (three) choices in the pretest, somehow learned along the way, and chose X in the posttest.

3.2 Polarisation: Identifying Forces Among Gender

One may recall from Sec. 2 that our student composition is female-dominated. As such, polarisation may be due to one gender alone; that is, possibly, due to females only. Let us look back at our main graph demonstrating polarisation namely, Fig. 4, and see if simple accounting supports this suspicion. At a glance, the wide separation between the solid lines and dashed lines both for pretest and posttest makes it highly unlikely unless otherwise, females far outnumber males which is not the case here; it is only 56% to 44%. The difference in the proportion of males and females (56% – 44% = 12%) is incommensurate

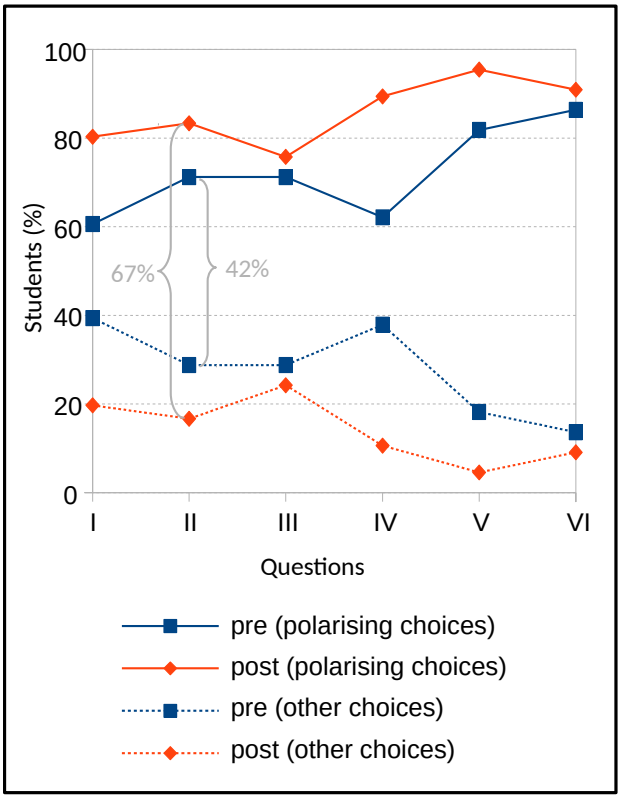

Figure 4: Distribution of students who selected the polarising choices (solid lines) over the other choices (dashed lines) in the six FCI questions I to VI.

with the wide gaps[7] in the pair of graphs for pretest and posttest shown in Fig. 4; for instance, for question II, we have a gap of 71% – 29% = 42% for the pretest and 83% – 17% = 67% for the posttest.

The possible gender aspect of polarisation can be seen more clearly by decomposing the graphs in Fig. 4 into contributions due to males and due to females. Figure 5 shows a gender-segregated distribution of student answers. We once again see the same characteristic exhibited in Fig. 4 indicating polarisation; that is, for each question, there is a *non-vanishing gap* in the pair of graphs for pretest and posttest. Needless to say, this observation holds for both males and females. Coupled with the argument elaborated in the first paragraph above, we then reach one of the main findings of this work—*polarisation is NOT unique to one gender*.

Having established this, we now move on to the question about the extent by which it is exhibited by one gender over the other. A visual inspection of the graphs (a) and (b) in Fig. 5 seems to indicate that males exhibit a more pronounced polarisation. To shed light on this issue, we introduce a quantitative measure called *degree of polarisation* P, defined as the difference between the percent of students who answered the polarising choices and those who elected the remaining choices. It has a minimum value of 0% indicating no polarisation, and a maximum value of 100% meaning all students elected the polarising choices. Geometrically, it is a measure of the gap between a pair of line graphs corresponding to polarising choices and other choices, symmetric about the horizontal line at the 50%-mark. (There are two of these pairs in Figs. 5(a) and 5(b) corresponding to pretest and posttest.) The narrower the gaps are, the smaller is the average value of P for all the six questions.

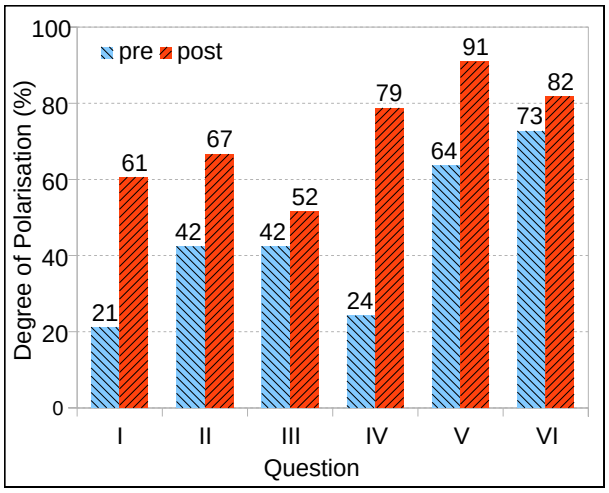

Figure 6: Degree of polarisation for all students on the FCI.

Figure 6 shows the degree of polarisation for all students irrespective of gender. We see a general pattern that P is higher for posttest than for pretest for all the six questions. We split this graph into contributions due to males and due to females (see Fig. 7) and then observe the same behaviour with females strictly following the pattern. However, on average, males exhibit a higher degree of polarisation for both pretest (56% versus 35% for females) and posttest (79% versus 66% for females) suggesting a possible gender gap. Such a gap may be interpreted in

[7]We formalise this notion of 'gap' as the degree of polarisation below.

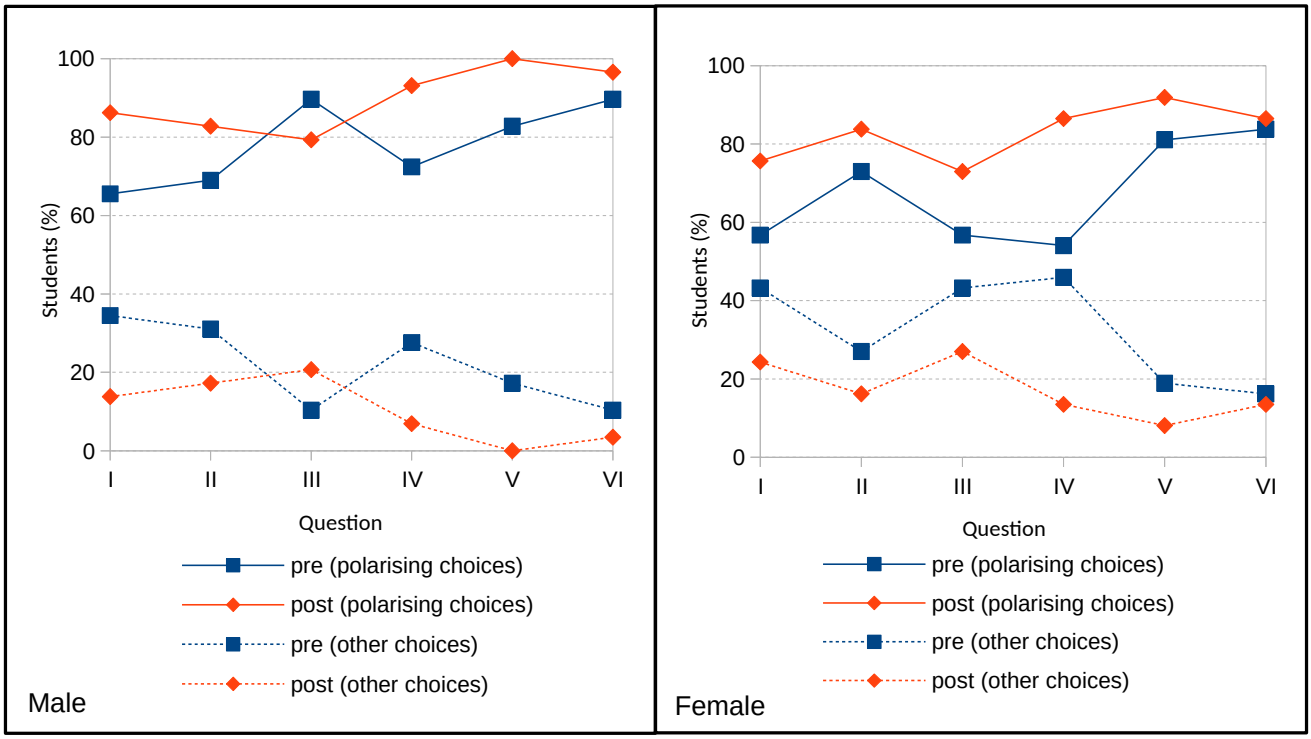

(a) (b)

Figure 5: Gender-segregated distribution for polarisation of student answers. The solid lines correspond to the polarising choices while the dashed lines refer to everything else. Moreover, the percent of students on the vertical axis correspond to their respective gender; that is, percent males among males in (a) and percent females among females in (b).

two ways. (In what follows, keep in mind that on average, males exhibit a higher degree of polarisation.) If a greater proportion of males happen to choose the wrong choice in the pair of polarising choices than that of females, then this may imply that males tend to be more confused. The possible gender gap may then be seen as in favour of females. On the other hand, if a greater proportion of males happen to choose the right choice in the pair of polarising choices than that of females, then this may imply that males tend to be more discerning about the correct set of forces acting on a given body. The possible gender gap may then be seen as in favour of males.

To resolve this issue, we need to establish if there really is a gender gap associated with the degree of polarisation in the first place. The two (possibly) interesting simulated scenarios we have just presented above can then only be taken into account if there actually is statistically significant (non-negligible) gender difference. This situation seems to demand a quantitative comparison test. A t-test involving P would be a viable candidate but as we have only six questions corresponding to six pairs of data points for males and females, this would yield a questionable result. On the other hand, one may see that from a slightly different perspective, we are dealing here with the question of the independence of two categories namely, (a) gender and (b) choice of answer (polarising choices and other choices). Treating all the polarisation-inducing questions on equal footing, we then find that if we count the frequency of students electing (a) polarising choices and (b) other choices, depending on gender, the appropriate test would be the chi-squared test, and this is what we use here.

For the pretest, our chi-squared test returns a p-value of 0.020. Since the p-value is less than 0.05, this suggests that at the 95% confidence level, we have statistically significant evidence that there is a gender aspect associated with polarisation. Looking back at Fig. 7(a), we see that it is not surprising at all. In five out of six questions, the P-bars for males are taller than that of females corresponding to an average of 56% versus 35%. Further examination of our data indicates that 39% (40%) of males (females) got the correct answer in the six questions. It follows that the greater degree of polarisation for males is due to the selection of the choice X in the pair of polarising choices. For the pretest, males seem to be more confused in identifying the correct set of forces acting on a given body.

For the posttest, our chi-squared test returns a p-value of 0.055. This means that at the 95% confidence level, we do not have statistically significant evidence suggesting a gender aspect of polarisation. With reference to Fig. 7(b) we see that although it exhibits the same pattern as that of Fig. 7(a), (that is, in five out of six questions, the P-bars for males are taller than that of females,) the relative difference in the degree of polarisation is smaller corresponding to an average P-value of 79% versus 66%. We may then say that along the way, students (males and females) learned more about forces and the polarisation gender gap observed in the pretest reduces posttest.

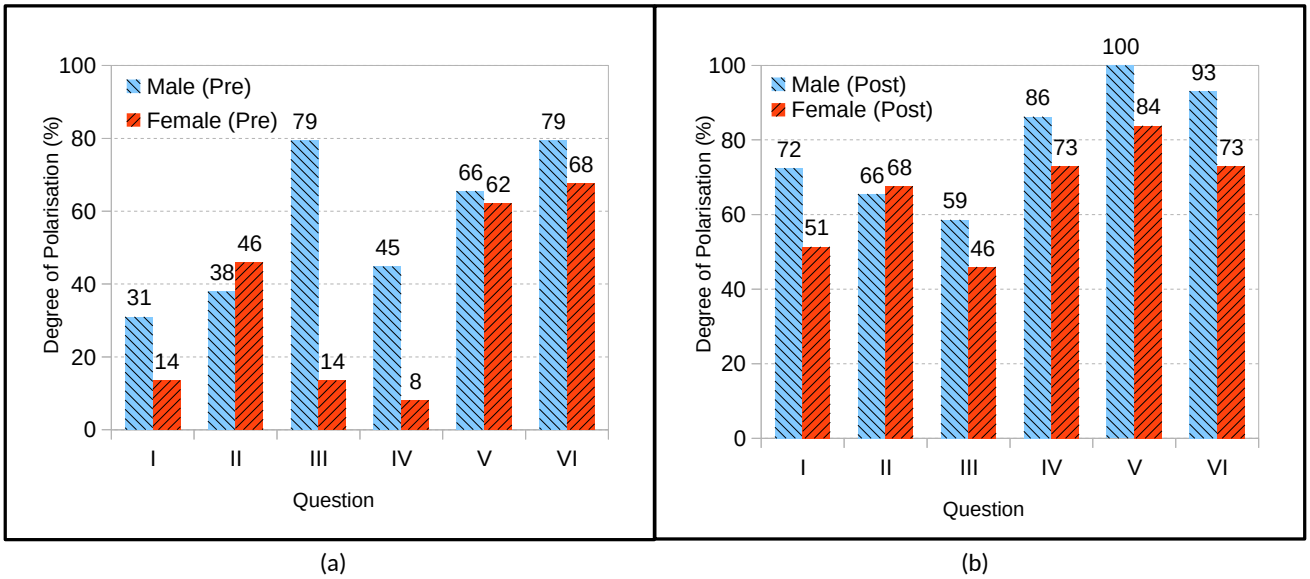

Figure 7: Gender-segregated distribution for the degree of polarisation.

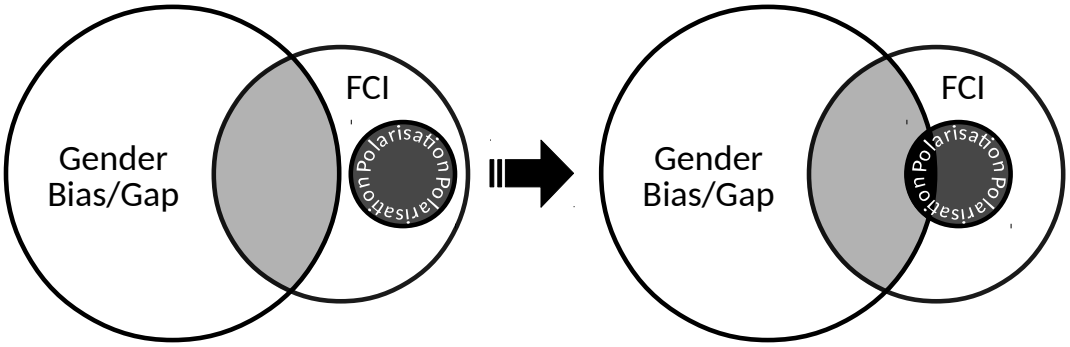

Figure 8: Venn diagram for polarisation, gender bias/gap, and the FCI. Our data suggest that polarisation does not have a serious gender dimension.

We are now in position to go back to the Venn diagram representing the place of polarisation in relation to gender gap and FCI. We have the following main findings:

- Polarisation is NOT unique to one gender.
- The gender gap that may have been attributed to the extent by which polarisation is exhibited pretest does not remain posttest (more data is possibly needed to give a more definitive answer for what we appear to have found pretest).

With these two points in hand, we move the circle for polarisation away from that of the gender gap/bias. As far as our results are concerned, it may not be placed completely outside of the zone for gender gap/bias as shown in Fig. 8, indicating that polarisation may have a gender dimension; albeit, something that fades with learning. Whether it will stay in this position (slightly) intersecting the circle for gender bias/gap, remains to be seen in future studies employing larger number of participants.

4 Concluding Remarks

Polarisation is a phenomenon wherein the addition of a 'fictitious' force to an otherwise correct set of forces causes a serious divide in the way students identify the valid set of forces acting on a given body. In this article, we have revisited this notion, this time, in relation to gender gap. Our data suggest that polarisation is not unique to one gender. Furthermore, the extent by which it is exhibited by males may differ at the beginning from that of females but the gap closes upon learning more about forces.

These findings involving the six polarisation-inducing questions in the FCI are complemented by our result for the FCI as a whole (see the appendix). We have discussed in this work evidence suggesting that there is no gender gap for global courses in conceptual physics. Although preliminary insight based on student means appeared to show a gender gap, using the t-test, we found that the null hypothesis was satisfied at the 95% confidence level; meaning, there is no statistically significant gender gap.

Our null result for the gender aspect of polarisation and FCI as a whole may require no justification at all.[8] However, in view of the existing evidences to the contrary for the FCI as a whole (see our references), it might be worth mentioning that our student participants were female-dominated and multi-racial in nature (international students). How these factors might have possibly influenced our result remains to be investigated.

As for future work, it is apparent that we would need a larger data set. Moreover, it would be beneficial to look at other international/global courses that have other inter-

[8] On a scale of 0 (not at all) to 4 (very much so), we asked our students the questions (1) 'Have you ever thought about or considered gender in physics?' and (2) 'Would you say that being female puts you at a disadvantage in physics?' We got an average of 1.2 in both questions from 33% of the students who responded to the survey, indicating an inclination towards the absence of gender gap/bias.

esting cohorts (not just the CBCMP program at Osaka University). Certainly, the study of whether or not 'stereotype threats' [20] affect performance in the international context warrants further investigation.

References

[1] I. A. Hallouin and D. Hestenes, Common sense concepts about motion, *Am. J. Phys.* **53**, 1043-1055, 1985.

[2] D. Hestenes, Who needs physics education research? *Am. J. Phys.* **(66)**, 465-467, 1998.

[3] D. Hestenes, M. Wells, and G. Swackhamer, Force Concept Inventory, *Phys. Teach.* **30**, 141-158, 1992.

[4] A. L. Alinea and W. Naylor, Polarization of physics on global courses, *Phys. Educ.* **50**, 210-217, 2015.

[5] Chemistry Biology Combined Major Program, Osaka University, `http://cbcmp.icou.osaka-u.ac.jp`

[6] A. T. Johnston and S. A. Southerland, A reconsideration of science misconceptions using ontological categories, *Annual Meeting of the National Association for Research in Science Teaching* (*New Orleans, Louisiana, April 2000*) on-line at `http://physics.weber.edu/johnston/research/ontological_categories_reconsidered.pdf`

[7] S. Bates et. al, Gender differences in conceptual understanding of Newtonian mechanics: a UK cross-institution comparison, *Euro. J. Phys.* **34** 421, 2013

[8] V. Coletta, Reducing the FCI Gender Gap, Physics Education Research Conference 2013, 101-104, 2013

[9] J. Docktor and K. Heller, Gender Differences in Both Force Concept Inventory and Introductory Physics Performance, *AIP Conf. Proc.* **1064** 15, 2008

[10] H. M. Glasser and J. P. Smith, On the vague meaning of gender in education research: the problem, its sources, and recommendations for practice, *Educ. Researcher* **37** 343, 2008.

[11] A. Madsen, S. B. McKagan and E. C. Sayre, Gender gap on concept inventories in physics: What is consistent, what is inconsistent, and what factors influence the gap? *Phys. Rev. Spec. Topics - Phys. Educ. Res.* **9** 020121, 2013

[12] Wikipedia contributors. Gender bias on Wikipedia. Wikipedia, The Free Encyclopedia. April 21, 2016, 02:17 UTC. Available at: `https://en.wikipedia.org/w/index.php?title=Gender_bias_on_Wikipedia&oldid=716313990`. Accessed April 21, 2016.

[13] A. P. Fagen, C. H. Crouch, and E. Mazur, Peer Instruction: Results from

a Range of Classrooms, *Phys. Teach*, **40**, 206-209, 2002.

[14] P. Heller, R. Keith, and S. Anderson, Teaching problem solving through cooperative grouping. Part 1: Group versus individual problem solving, *Am. J. Phys.* **60**(7), 627-636, 1991.

[15] Smith, M. K., W. B. Wood, W. K. Adams, C. Wieman, J. K. Knight, N. Guild, and T. T. Su. Why Peer Discussion Improves Student Performance on In-Class Concept Questions. *Science*, 323, 122-24, 2009.

[16] MasteringPhysics, Pearson Publishing Group, `http://www.pearsonmylabandmastering.com/masteringphysics/`

[17] M. J. Crawley, Statistics: An Introduction Using R (2nd ed), Wiley, West Sussex UK (2014).

[18] T. C. Urdan, Statistics in Plain English (3rd ed), Routledge, New York USA (2010)

[19] R Foundation `www.r-project.org/`

[20] J. R. Shapiro and A. M. Williams, The Role of Stereotype Threats in Undermining Girls and Womens Performance and Interest in STEM Fields, *Sex Roles* **66** 175, 2012.

[21] R. R. Hake, Interactive-engagement versus traditional methods: a six-thousand-student survey of mechanics test data for introductory physics courses, *Am. J. Phys.* **66** 64-74, 1998

[22] V. P. Coletta and J. A. Phillips, Interpreting FCI scores: Normalized gain, preinstruction scores, and scientific reasoning ability, *Am. J. Phys.* **73**, 1172-1182, 2005

[23] V. Cahyadi, The effect of interactive engagement teaching on student understanding of introductory physics at the faculty of engineering, University of Surabaya, Indonesia, *Higher Education Research Development*, **23**(4) 454 464, 2004.

[24] S. Freeman, et al., Active learning increases student performance in science, engineering, and mathematics, *Proceedings of the National Academy of Sciences*, **111**(23) 8410-8415, 2014.

[25] F. Ornek and M. Orbay, Activity-based Interactive Engagement in Science (Physics) Laboratory: An Approach to Stimulate Pre-Service Teachers' Conceptual Understanding, *Physics Education*, **28**(2), 2012.

A Appendix: The FCI as a Whole

Although this work mainly focuses on the gender aspect of polarisation, it would not be a complete study without mentioning the result of the FCI as a whole. The point in elaborating this is not to repeat what has been

found out in the literature; that is, there is gender gap associated with the FCI considered as a whole. In fact, as we shall see, we are part of the minority that deviates from this finding. The additional point then, aside from completeness, is to some extent, a sense of *complementarity*. Our analysis and elaboration below serve to support the idea that polarisation is not a gender-specific phenomenon and the extent by which it is exhibited by students does not have a serious gender aspect.

A.1 Results and Analysis

Table 1 shows the results of the FCI for four batches of entrants (from AY 2011-12 to AY 2014-15)[9] corresponding to a total of 66 students, for pretest and posttest. The mean scores for the pretest and posttest are 52% and 62% respectively, corresponding to a rise of about 20%. Our (paired) t-test returns a p-value of 2.9×10^{-8}. This indicates that at the 95% confidence level, the null hypothesis[10] was not satisfied and suggests the results do lead to a positive increase in the post scores.

The t-test can only indicate whether there is a statistically significant difference between the pretest and posttest scores. A good measure commonly employed in studies like this to quantify the improvement with respect to the score in the pretest, is provided by the normalized gain, G [21]. It is defined as the difference between the posttest and pretest scores divided by the maximum possible rise in score relative to the pretest result. Symbolically,

$$G = \frac{\langle \%S_f \rangle - \langle \%S_i \rangle}{100\% - \langle \%S_i \rangle},$$

where $\%S_f$ and $\%S_i$ are the final and initial scores in percent respectively.

Also included in Table 1 are the G-values for each AY for the four batches of students. On average, we find a relatively low value of $G = 0.20$ (see ref. [22] for the interpretation of FCI scores). This is in spite of the use of interactive engagement [21, 23, 24, 25] in the form of (a) peer discussion and (b) use of MasteringPhysics^{TM} with the guidance of the instructor/teaching assistant. As we previously argued [4], the corrective measure built into MasteringPhysics^{TM} might have contributed in the low normalized gain. In addition to this, the formal contact hours between students and teacher (one meeting per week each lasting for only 1.5 hours, as stated in Sec. 2) might have been not enough to instil mastery of the core concepts in Newtonian mechanics.

A.2 Gender Differences?

Table 2 is a summary table comparing the performance of males and females in the pretest and posttest. Our data suggest that considering the mean scores, males tend to perform better on both the pretest and

[9] This is an updated set of data a part of which (AY 2011-12 to AY 2013-14) we previously presented in ref. [4].

[10] In this case the null hypothesis is that there is no statistically significant gain between post and pre test scores.

Table 1: FCI results (in percent) for four academic years starting from 2011 and ending 2015. The number n under each academic year indicates the number of students while the quantity SD stands for standard deviation.

Group	2011-2012 $n = 11$	2012-2013 $n = 18$	2013-2014 $n = 18$	2014-2015 $n = 19$	Total $N = 66$
	Mean (SD)	Mean (SD)	Mean (SD)	Mean (SD)	Mean (SD)
Pretest(%)	57 (22)	55 (25)	49 (22)	50 (22)	52 (23)
Posttest(%)	67 (23)	66 (21)	55 (23)	62 (19)	62 (21)
Gain	0.24	0.23	0.12	0.25	0.20

posttest. This observation is further supported by a higher G-value indicating a greater improvement on the part of the males. Looking at the table, a difference of $\Delta G = 0.23 - 0.18 = 0.05$ might not seem much but compared to the average ($G_{\mathbf{ave}} = 0.21$), this leads to a relatively large percent difference of 24%. Having laid down the means and G-value, let us see if our preliminary insight can survive rigorous statistical testing.

Table 2: FCI results (in percent) for female and male participants from AY 2011-12 to AY 2014-15. The heading % Diff means percent difference while the labels Pre and Post correspond to Pretest and Posttest respectively.

Group	Female $n = 37$	Male $n = 29$	% Diff
	Mean (SD)	Mean (SD)	
Pre(%)	49 (22)	57 (22)	16
Post(%)	58 (21)	67 (21)	15
Gain	0.18	0.23	24

Pretest. At the 95% confidence level, or $\alpha = 0.05$, we find that $p = 0.13 > \alpha$, so there is no significant difference between the means of the pretest scores of males ($x_{\mathrm{m,pre}} = 57\%$) and females ($x_{\mathrm{f,pre}} = 49\%$). Though the percent difference between the means may not be ignored at 16% in favour of males, the relatively wide variation of student scores (as measured by the standard deviation) leads to acceptance of the null hypothesis via the t-test.

Posttest. At the 95% confidence level, or $\alpha = 0.05$, we find that $p = 0.087 > \alpha$, so there is no significant difference between the means of the posttest scores of males ($x_{\mathrm{m,post}} = 67\%$) and females ($x_{\mathrm{f,post}} = 58\%$). Though the percent difference between the means may not be ignored at 15% (only 1% away from that of the pretest), the relatively wide variation of student scores (as measured by the standard deviation) leads to acceptance of the null hypothesis via the t-test.

It is worth noting that our *preliminary insight* above is in agreement with the review article [11] on gender gap involving the FCI to the extent that male average score and G-value are higher than that of female. However, in our case, the difference in means in

favour of males is not supported by the t-test results; the fluctuation in student scores is large enough to prevent us concluding that there is indeed a gender gap.

Recalling the gender distribution of the participants mentioned in Sec. 2, we find that it is female-dominated (56% vs. 44%). In view of ref. [20], the absence of 'stereotype threat' might have been one of the possible factors leading to a statistically null gender difference.[11] Furthermore, the fact that majority of our students are international students, their global mindset might correspond to the absence of the gender dimension. Although these are interesting angles to look at, owing to the limited space for this work, we leave the investigation for future studies.

Our result above brings us back to the gender aspect of polarisation. Had there been a statistically significant gender difference in the FCI performance as a whole, polarisation would have been expected to follow suit. In theory (with polarisation-inducing questions constituting 20% of all the questions), it is possible that the gender aspect of the two to be opposite each other (one with gender gap while the other has none). What we have found out is that both genders exhibit it. Moreover, the gender aspect associated with the degree of polarisation seems to fade naturally as students learn more about forces. Except for the possible preliminary gender difference, the null result for the FCI as a whole complements our main findings about polarisation.

[11] This sort of justification seems unnecessary as far as the null result is concerned. However, in view of the overwhelming data on gender gap presented in ref. [11], we find it good to find some words to somehow support our result.

Each normalized state is a member of an orthonormal basis: A simple proof

Iman Sargolzahi[1] and Ehsan Anjidani[2]

[1]Department of Physics, University of Neyshabur,
P. O. Box 91136-899, Neyshabur, Iran
sargolzahi@neyshabur.ac.ir

[2]Department of Mathematics, University of Neyshabur,
P. O. Box 91136-899, Neyshabur, Iran.
anjidani@neyshabur.ac.ir

(Submitted 24-01-2016)

Abstract

In a finite dimensional Hilbert space, each normalized vector (state) can be chosen as a member of an orthonormal basis of the space. We give a proof of this statement in a manner that seems to be more comprehensible for physics students than the formal abstract one.

1 Introduction

Finite dimensional Hilbert spaces, e.g. spin of a particle or polarization of a photon, is of great interest in quantum mechanics, specially in quantum information and computation theory [1]. So, studying the mathematical properties of such spaces is necessary for physics students, specially in graduate levels.

One useful result in a finite dimensional Hilbert space is that an arbitrary normalized state can be chosen as a member of an orthonormal basis of the space. In the linear algebra theory, this statement is proven [2]: A set including only one state, constructs a linearly independent set. But this proof seems rather abstract, at least, for physics students. So in this paper, instead, we prove this statement by constructing directly a basis including our arbitrarily chosen state. Doing so, in a two dimensional Hilbert space (one-qubit state space), is simple using the Bloch sphere. Then, by induction, we generalize this result to the higher finite dimensional Hilbert spaces too. We hope that this method be more comprehensible for physics students.

The paper is organized as follows: In the next section, we review the properties of vector spaces briefly. In section 3, using the Bloch sphere, it is shown that in the one-qubit case, each state is a member of an orthonormal basis. Our main result is given in section 4, in which, by induction, we generalize the result of section 3 to arbitrary finite dimensional spaces. In section 5, we discuss the consequences of this result briefly. When our result can be used for the countable infinite dimensional case is the subject of section 6 and, finally, our paper is ended by a summary in section 7.

2 Finite dimensional vector spaces

A vector space V on complex numbers C is a set of elements, like $a, b, c, \cdots$, which we call them vectors and satisfy two following properties [1] [3]:

1. Sum of each two vectors a and b of V is also a vector in V like c:

$$a \in V,\ b \in V \Rightarrow a + b = c \in V. \qquad (1)$$

2. Multiplication of a vector a by a complex number (scalar) z, is also a member of V:

$$a \in V,\ z \in C \Rightarrow za \in V. \qquad (2)$$

Two above properties are obviously the generalization of the properties of real vectors in the three dimensional space:

1. Sum of two vectors $\mathbf{A}$ and $\mathbf{B}$ is also a vector like $\mathbf{C}$.

2. Multiplication of a vector $\mathbf{A}$ by a real scalar c is also a vector (parallel to $\mathbf{A}$).

In addition, in a vector space there is a zero vector, which we denote by 0, with the property

$$a + 0 = a \qquad \text{for any } a \in V. \qquad (3)$$

[1] For more detailed definition of a vector space see e.g. [2, 3, 4]

By definition, a set of nonzero vectors $\{a_1, \cdots, a_n\}$ are linearly independent if the equality

$$z_1 a_1 + \cdots + z_n a_n = 0 \tag{4}$$

(with $z_i \in C$, $i = 1, \cdots, n$) is satisfied only when for all $1 \leq i \leq n$, $z_i = 0$. Assume that the maximum number of linearly independent vectors in the vector space V is a finite number $n < \infty$. Now, consider the following equality, in which the vector b is also nonzero:

$$z_1 a_1 + \cdots + z_n a_n + zb = 0. \tag{5}$$

Obviously, the above equation has a trivial solution: $z_i = 0$, $(i = 1, \cdots, n)$ and $z = 0$. If there were no other solution except the trivial one, then $\{a_1, \cdots, a_n, b\}$ would be a linearly independent set with $(n+1)$ members, which is in contradiction to our assumption. So, equation (5) has another solution; i.e. at least one of z_i and also z are nonzero. This has an important consequence: For each $b \in V$, we have

$$\begin{aligned} b &= \frac{z_1}{-z} a_1 + \cdots + \frac{z_n}{-z} a_n \\ &= \sum_{i=1}^{n} c_i a_i, \end{aligned} \tag{6}$$

where $c_i := \frac{z_i}{-z}$. In other words, any vector in the vector space V can be written as a linear combination of vectors $a_1, \cdots, a_n$. The set $\{a_1, \cdots, a_n\}$ is called a basis for the vector space V. Such a vector space, in which the number of the basis vectors is finite $(n < \infty)$, in other words, the maximum number of linearly independent vectors is finite, is called a finite dimensional (n-dimensional) vector space [2, 3].

A finite dimensional vector space V equipped with an inner product is called a Hilbert space or an inner product space [1]. A function $(.,.)$ from $V \times V$ to C is an inner product if it satisfies the following properties [1, 3, 4]:

1. $(.,.)$ is linear in the second argument (λ_i are complex numbers.):

$$\left(a, \sum_{i=1}^{m} \lambda_i b_i\right) = \sum_{i=1}^{m} \lambda_i (a, b_i). \tag{7}$$

2. For any $a, b \in V$,

$$(a, b) = (b, a)^*. \tag{8}$$

3. For any $a \in V$,

$$(a, a) \geq 0, \tag{9}$$

where the equality occurs if and only if $a = 0$.

We define the norm of a vector a by

$$\|a\| = \sqrt{(a, a)}. \tag{10}$$

If $\|a\| = 1$, then we say that a is a normalized vector. In addition, if

$$(a, b) = 0, \tag{11}$$

then we say that the two vectors a and b are orthogonal.

Following the Gram-Schmidt procedure [3, 4], one can construct an orthonormal basis $\{e_1, \cdots, e_n\}$ from the basis $\{a_1, \cdots, a_n\}$ in an

inner product space. The orthonormality of vectors e_i means that $(e_i, e_j) = \delta_{ij}$, where δ_{ij} is the Kronecker delta function ($\delta_{ij} = 0$ for $i \neq j$ and $\delta_{ij} = 1$ for $i = j$). The Gram-Schmidt procedure is as follows:

$$e_1 := \frac{a_1}{\|a_1\|}, \tag{12}$$

and for each $2 \leq i \leq n$,

$$e_i := \frac{e_i'}{\|e_i'\|}, \tag{13}$$

where

$$e_i' := a_i - \sum_{j=1}^{i-1} (e_j, a_i) e_j. \tag{14}$$

It is easy to see that the set $\{e_1, \cdots, e_n\}$ is orthonormal. In addition, since according to (12), (13) and (14) we can write each a_i in terms of vectors e_j, for each $b \in V$ we have

$$b = \sum_{i=1}^{n} c_i a_i = \sum_{i=1}^{n} d_i e_i, \tag{15}$$

where the coefficients d_i are complex numbers. We may use the column matrix notation for the orthonormal basis vectors e_i:

$$e_1 = \begin{pmatrix} 1 \\ 0 \\ \vdots \\ 0 \end{pmatrix}_{n\times 1} , \quad \cdots \quad , e_n = \begin{pmatrix} 0 \\ \vdots \\ 0 \\ 1 \end{pmatrix}_{n\times 1} . \tag{16}$$

Hence, for each $b \in V$ we have

$$b = \sum_{i=1}^{n} d_i e_i = d_1 \begin{pmatrix} 1 \\ 0 \\ \vdots \\ 0 \end{pmatrix} + \cdots + d_n \begin{pmatrix} 0 \\ \vdots \\ 0 \\ 1 \end{pmatrix} = \begin{pmatrix} d_1 \\ \vdots \\ d_n \end{pmatrix}. \tag{17}$$

Now, using the properties (7) and (8) of the inner product function, it can be shown that for any $v, w \in V$, where

$$v = \begin{pmatrix} v_1 \\ \vdots \\ v_n \end{pmatrix} \quad , \quad w = \begin{pmatrix} w_1 \\ \vdots \\ w_n \end{pmatrix},$$

we have [1]

$$(v, w) = \begin{pmatrix} v_1^* & \cdots & v_n^* \end{pmatrix} \begin{pmatrix} w_1 \\ \vdots \\ w_n \end{pmatrix} = \sum_{i=1}^{n} v_i^* w_i. \tag{18}$$

We can continue the above discussion and introduce linear operators on V, their matrix representation and ... [1, 5].

Let's come back to our question: whether an arbitrary normalized vector $b \in V$ can be chosen as a member of an orthonormal basis. As we mentioned, the answer is yes, since the set $\{b\}$ is a linearly independent set. Therefore b is the basis vector of a one dimensional subspace of V and so a basis vector of the V itself [2]. In addition, one can find exactly $n-1$ other nonzero vectors w_i in such a way that $\{b, w_1, \cdots, w_{n-1}\}$ constructs a linearly independent set and so a basis for V (see [2, 3]). Equipped with the linearly independent set $\{b, w_1, \cdots, w_{n-1}\}$ and using the Gram-Schmidt procedure, we can construct the orthonormal basis $\{v_1 (= b), v_2, \cdots, v_n\}$ for V, and therefore the proof is completed.

The above discussion, though is satisfying for a mathematician, may be rather abstract for a physics student. So, instead, we prove that each normalized vector b is a member of an orthonormal basis, by constructing such

a basis directly from the orthonormal computational basis $\{e_1, \cdots, e_n\}$. This can be done simply for the two dimensional case, i.e. qubits, using the Bloch sphere. For the completeness of our discussion, we give this result in the next section and then in section 4, we generalize it to the higher dimensional cases.

3 Two dimensional Hilbert space: one-qubit state space

In a two dimensional Hilbert space, according to (15), each (normalized) state can be written as:

$$\psi = \alpha 0 + \beta 1, \tag{19}$$

where we use the notation 0 and 1 for the orthonormal computational basis, instead of e_1 and e_2. Decomposition coefficients α and β are (in general) complex numbers. Since ψ is normalized, from (10) and (18) we have

$$|\alpha|^2 + |\beta^2| = 1. \tag{20}$$

So, we can write (19) as follows

$$\psi = e^{i\gamma}\left(\cos\frac{\theta}{2}0 + e^{i\varphi}\sin\frac{\theta}{2}1\right), \tag{21}$$

where $i = \sqrt{-1}$ and γ, θ, φ are real numbers. Comparing (19) and (21), we have

$$\alpha = e^{i\gamma}\cos\frac{\theta}{2} \quad , \quad \beta = e^{i(\gamma+\varphi)}\sin\frac{\theta}{2};$$

so (20) is obviously satisfied. Therefore, up to phase factor, we can write each ψ as [1]:

$$\psi = \cos\frac{\theta}{2}0 + e^{i\varphi}\sin\frac{\theta}{2}1 \qquad (0 \le \varphi \le 2\pi). \tag{22}$$

Obviously, choosing φ out of the above interval does not give us any new state. Also, it can be shown that choosing $0 \le \theta \le \pi$ covers all possible states; i.e. if we choose θ out of this interval, then, up to a phase factor, it coincides with a state with $0 \le \theta \le \pi$.
So, all possible one-qubit states can be written as follows:

$$\psi = \cos\frac{\theta}{2}0 + e^{i\varphi}\sin\frac{\theta}{2}1 \qquad (0 \le \varphi \le 2\pi,\ \ 0 \le \theta \le \pi). \tag{23}$$

Therefore, we can relate each state in a two dimensional Hilbert space to a point on a unit three dimensional sphere, called the Bloch sphere [1].

Now, consider an arbitrary state ψ_0 (with $\theta = \theta_0$ and $\varphi = \varphi_0$):

$$\psi_0 = \cos\frac{\theta_0}{2}0 + e^{i\varphi_0}\sin\frac{\theta_0}{2}1. \tag{24}$$

It is easy to show that ψ_0 is a member of an orthonormal basis for our one-qubit state space. Consider the state ϕ_0 (with $\theta = \pi - \theta_0$ and $\varphi = \varphi_0 + \pi$):

$$\phi_0 = \cos\frac{\pi-\theta_0}{2}0 + e^{i\varphi_0}\sin\frac{\pi-\theta_0}{2}1 = \sin\frac{\theta_0}{2}0 - e^{i\varphi_0}\cos\frac{\theta_0}{2}1. \tag{25}$$

Using (18), it is easy to show that ψ_0 and ϕ_0 are orthonormal. In addition, we have

$$\begin{aligned} 0 &= \cos\frac{\theta_0}{2}\psi_0 + \sin\frac{\theta_0}{2}\phi_0, \\ 1 &= e^{-i\varphi_0}\left(\sin\frac{\theta_0}{2}\psi_0 - \cos\frac{\theta_0}{2}\phi_0\right). \end{aligned} \tag{26}$$

So, we can decompose each state ψ, in this two dimensional state space, in terms of ψ_0 and ϕ_0. This can be done by inserting 0 and 1 from (26) in (19). Therefore, $\{\psi_0, \phi_0\}$ is an orthonormal basis for one-qubit state space, which includes our arbitrarily chosen state ψ_0.

4 Higher dimensional Hilbert spaces

Now we want to generalize the result of the previous section to an arbitrary finite dimensional Hilbert space. We begin with the three dimensional case: one-qutrit state space.

An arbitrary one-qutrit state can be decomposed in terms of the computational basis $\{0, 1, 2\}$ as follows

$$\omega = \alpha' 0 + \beta' 1 + \gamma' 2, \tag{27}$$

where α', β', γ' are complex numbers. The normality condition is as follows

$$|\alpha'|^2 + |\beta'|^2 + |\gamma'|^2 = 1. \tag{28}$$

We want to show that the arbitrary state ω is a member of an orthonormal basis. We do this by constructing such a basis explicitly. (We restrict ourselves to the case $\alpha', \beta', \gamma' \neq 0$, otherwise, the problem reduces to the lower dimensional cases.) Consider the projection of ω into the subspace spanned by $\{0, 1\}$:

$$\psi' = \alpha' 0 + \beta' 1. \tag{29}$$

So

$$\psi = \frac{\alpha'}{\psi'} 0 + \frac{\beta'}{\psi'} 1 := \alpha 0 + \beta 1 \quad (\psi' := \|\psi'\|) \tag{30}$$

is a normalized vector in this two dimensional subspace. ψ is obviously in the form of (19). So, up to phase factor, it can be written as (24) and we can find an orthogonal state to ψ as (25):

$$\varphi = \beta^* 0 - \alpha^* 1. \tag{31}$$

(Note that φ is also orthogonal to ω.) Now, we can write (27) as:

$$\omega = \psi' \psi + \gamma' 2, \tag{32}$$

where ψ and 2 are orthonormal. So, ω in (32) is also in the form of (19) which again can be written as (24) and we can find an orthogonal state to it as (25):

$$\nu = \gamma'^* \psi - \psi' 2; \tag{33}$$

note that $\psi' = \|\psi'\|$ is a positive number. Now it is obvious that the set $\{\varphi, \omega, \nu\}$ is an orthonormal set. Also an arbitrary state

$$a = \alpha_0 0 + \alpha_1 1 + \alpha_2 2$$

in this one-qutrit state space, can be decomposed in terms of $\{\varphi, \omega, \nu\}$: similar to (26), we can write 0 and 1 in terms of ψ in (30) and φ in (31) and then we can write ψ and 2 in terms of ω in (32) and ν in (33). So, we can write a in terms of φ, ω and ν.

In summary, $\{\varphi, \omega, \nu\}$, including our arbitrarily chosen state ω, constructs an orthonormal basis for three dimensional Hilbert space.

Also note that φ and ν span a two dimensional subspace, like 0 and 1 in (19). So, similar to the previous section, instead of φ and ν, we can choose any other two orthonormal

states φ' and ν' which also span this subspace. Since φ' and ν' are written in terms of φ and ν, the vectors φ' and ν' are orthogonal to ω. Therefore, the set $\{\omega, \varphi', \nu'\}$ is also an orthonormal basis for one-qutrit state space.

In other words, in a three dimensional Hilbert space (and also in higher dimensional cases) in contrast with the two dimensional one, we can find an infinite number of orthonormal bases including our chosen state ω.

In the two dimensional Hilbert space, for each ψ_0 in (24), up to a phase factor, there is only one ϕ_0 in (25) such that the set $\{\psi_0, \phi_0\}$ constructs an orthonormal basis including ψ_0.

Generalization of our result to the higher dimensions can be done by induction: Assume that in an n-dimensional Hilbert space, each arbitrary state is a member of an orthonormal basis. We want to show that it is also true for $(n+1)$-dimensional Hilbert space.

Let's show the computational basis as $\{1, 2, \cdots\}$. So, in $(n+1)$-dimensional state space, we can decompose an arbitrary state ω as

$$\omega = \sum_{i=1}^{n+1} c'_i i, \tag{34}$$

where all c'_i are complex numbers and the normality condition is as follows

$$\sum_{i=1}^{n+1} |c'_i|^2 = 1. \tag{35}$$

We suppose that all c'_i are nonzero, otherwise the problem reduces to the lower dimensional cases.

Now, consider the projection of ω into the n-dimensional subspace spanned by $\{1, \cdots, n\}$:

$$\psi' = \sum_{i=1}^{n} c'_i i. \tag{36}$$

Hence

$$\psi = \frac{\psi'}{\psi'} = \sum_{i=1}^{n} \frac{c'_i}{\psi'} i := \sum_{i=1}^{n} c_i i, \qquad (\psi' := \|\psi'\|), \tag{37}$$

is a normalized vector in this n-dimensional subspace. Since in the n-dimensional Hilbert space each state is a member of an orthonormal basis, we can find $n-1$ states φ_i such that $\{\varphi_1, \cdots, \varphi_{n-1}, \psi\}$ constructs an orthonormal basis of the n-dimensional subspace spanned by $\{1, \cdots, n\}$. Thus, $\{\varphi_1, \cdots, \varphi_{n-1}, \psi, n+1\}$ is an orthonormal basis of the $(n+1)$-dimensional Hilbert space.

In addition, we have

$$\omega = \psi'\psi + c'_{n+1} n + 1. \tag{38}$$

States ψ and $n+1$ span a two dimensional subspace which also can be spanned by orthonormal states ω and

$$\nu = c'^{*}_{n+1}\psi - \psi' n + 1. \tag{39}$$

Therefore the set $\{\varphi_1, \cdots, \varphi_{n-1}, \omega, \nu\}$, including the arbitrary state ω, is an orthonormal basis of $(n+1)$-dimensional state space and the proof is completed.

5 Consequences

In the previous section, we proved that in a finite dimensional state space, an arbitrary

state ω can be chosen as a member of an orthonormal basis. It seems valuable to discuss briefly the consequences of this result.

The first consequence of the above result is that, in addition to the computational basis, there exist other orthonormal bases for a finite dimensional state space. It has an important consequence: existence of unitary operators. A unitary operator U is an operator satisfying the following relations [5]:

$$UU^\dagger = I \qquad , \qquad U^\dagger U = I, \tag{40}$$

where $U^\dagger$ is the adjoint of U and I is the identity operator. Now if we consider two orthonormal bases $\{1, \cdots, n\}$ and $\{\varphi_1, \cdots, \varphi_n\}$ for an n-dimensional Hilbert space, then it can be shown simply that

$$U = \sum_{i=1}^{n} \varphi_i i \tag{41}$$

is a unitary operator [5].

Also, using this fact that each state can be chosen as a member of an orthonormal basis, one can prove the Cauchy-Schwarz inequality, as given in [1].

6 Countable infinite dimensional Hilbert spaces

Till now, our discussion was restricted to the finite dimensional Hilbert spaces, which are used widely in quantum information and computation theory [1]. However, countable infinite dimensional Hilbert spaces are also of interest in quantum theory. Standard examples in this context are the harmonic oscillator and the infinite well [6].

Proving, in the general case, that an arbitrary normalized state ω, in a countable infinite dimensional Hilbert space V, is a member of an orthonormal basis of V, is out of the scope of this paper. But, there is an important special case for which we can prove the above statement simply, using our result in section 4.

Assume that the set $\{1, 2, \cdots\}$ is the orthonormal computational basis of our countable infinite dimensional Hilbert space V. So we can write each $\psi \in V$ as

$$\psi = \sum_{i=1}^{\infty} c_i i, \tag{42}$$

where c_i are complex numbers. Now, consider the special case that our arbitrarily chosen state ω can be written as

$$\omega = \sum_{i=1}^{N} \alpha_i i, \tag{43}$$

where N is a finite positive integer. Therefore, ω belongs to a finite dimensional subspace of V, spanned by $\{1, 2, \cdots, N\}$. Let's denote this subspace as V'. Now, using the result of section 4, we can find an orthonormal basis for V' which includes ω: $\{\omega = e_1, e_2, \cdots, e_N\}$. So, the whole V can be spanned by the orthonormal basis $\{\omega = e_1, e_2, \cdots, e_N, N+1, N+2, \cdots\}$, which includes our chosen state ω.

7 Summary

In a finite dimensional Hilbert space, each normalized state can be chosen as a member of an orthonormal basis of the space. Instead of the formal proof of this statement, we give a simple proof by constructing such a basis directly. In two dimensional case, this can be done by using the Bloch sphere. We generalize the two dimensional case to the higher dimensional state spaces by induction. We hope that our proof be more clear for physics students than the formal one.

In addition, even when the Hilbert space is countable infinite dimensional, we can use the above result, for an important special case, given in section 6.

Acknowledgments

We would like to thank an anonymous referee for his (her) suggestion to add a section about the infinite dimensional case.

References

[1] M. A. Nielsen and I. L. Chuang, *Quantum Computation and Quantum Information* (Cambridge University Press, 2000).

[2] K. Hoffman and R. Kunze, *Linear Algebra* (Prentice-Hall, 1971) Chap. 2.

[3] S. Hassani, *Foundations of Mathematical Physics* (McGraw-Hill, 1991) Chap. 2.

[4] A. W. Joshi, *Matrices and Tensors in Physics* (John Wiley and Sons, 1995) Chap. 1.

[5] J. J. Sakurai and J. Napolitano, *Modern Quantum Mechanics* (Addison-Wesley, 2011) Chap. 1.

[6] S. Gasiorowicz, *Quantum Physics* (John Wiley and Sons, 2003).

A Study of the Effect of Figure of Merit on the Performance of FTO Based Organic Light Emitting Diode (OLED)

D. Saikia* and R. Sarma

Thin Film Lab. Dept of Physics,
J.B.College, Jorhat, Assam,
India. Pin code: 785001,
Ph. No. : 8011468483, Fax :(0376)2300605

*Corresponding Author: dhrubajun@gmail.com

(*Submitted*: 08-09-2016)

Abstract

Organic Light Emitting Diodes have been fabricated and study their J-V-L performances. Here N,N'-bis (3- methyl phenyl)- N, N' (phenyl)-benzidine (TPD) is used as hole transport layer(HTL) and Tris(8-hydroxy quinolinato) aluminium (Alq_3) as both emitting layer and electron transport layer(ETL). The performance of the devices explains on the basis of figure of merit (FOM) which is the function of optical transmittance and sheet resistance. The range of thicknesses of hole transport layer is 10nm-50nm and that of emissive layer is 15nm-70nm respectively. Here high luminance has been obtained at the operating voltage less than 20 volt with turn-on voltage 6.7 volt. The performances of the devices are studied by J-V and L- V characteristics. With a combination of 30nm HTL and 44nm ETL organic layer thickness, better charge balancing is achieved and luminous efficiency is maximum. This bilayer organic film provides maximum luminance greater than 2500 Cd/m^2 with a current density 144 mA/cm^2.

1. Introduction

Organic light emitting diode (OLED) is based on the principle of Electro luminance (EL). This is made by placing a thin film of an organic material between two conductors of different work function. When a voltage is applied, electron and hole are injected into the EL material. When these recombine, light is emitted. The organic layers are highly disordered, amorphous in form and consist of molecular energy levels- the highest occupied molecular orbital (HOM U) and the lowest unoccupied molecular orbital (LUMO). Appropriate selection of anode and cathode materials should be such that their work functions values are closely match the HOMO & LUMO levels respectively. ITO films fabricated on glass substrate are widely adopted as transparent anodes. There are some reports on OLED with polymer anode but also supported by ITO glasses because the thickness and weight of the devices are dominated by the supporting substrate [1, 2, 3]. Tremendous progress has been made in the resent years. OLED technology is expected to show great impact on the future of lighting application & flat panel display [4, 5]. Because of the suitable properties of Alq3, it is widely used in OLED [6]. Philip R. Dravian developed the bilayer cathode

OLED on Alq3 based devices. Haichuan Mu et. al. study the film morphology with deposition rate Alq3 based organic luminescent devices [7]. N. Thejo & S.J. Dhoble fabricate the ALQ3 based OLED using Eu x $Y_{(1-x)}$ $(TTA)_3$ phen organic complexes [8]. G. Luka et al. study the properties of ALQ3 OLED with undoped zinc-oxide anode layer [9]. Recently L. Zhou et al. developed the improved Alq3 based OLED using bilayer anode combination of Al_2O_3 and ITO [10]. However although the different study of OLED is available in the literature but all of them are ITO related, only few reports are found on FTO [11, 12]. Here in this paper we report an Alq3 based Organic Light Emitting Diode (OLED) with optimize thickness region of HTL and light emitting layer in which luminance is greater than 2500 Cd/ m^2 with turn on voltage less than 10 volt.

2. Experimental Details

In our experiments Fluorine doped tin oxide (FTO) coated glasses are subjected to a routine cleaning procedure prior to the loading into the evaporator. N, N'- bis (3-methyl phenyl)- N, N' (phenyl)-benzidine(TPD) and Tris(8-hydroxy quinolinato) aluminium (Alq_3) are used as hole transport layer and the electron transport/emissive layer respectively. OLED with the structure FTO/TPD/Alq3/ LiF/A L is deposited by thermal evaporation unit (MODEL VT - 2015). The film thickness and deposition rate of the organic films and cathode layer were recorded by thickness monitor (MODEL DTM-10). The FTO coated glasses are patterned by using etching technology. All the films are deposited at the base pressure of 5×10^{-5} Torr with deposition rate greater than 12Å/sec. The J-V and L-V characteristics were measured by digital source-meter unit (SM U) and the Luminance meter unit. The transmittance spectra of

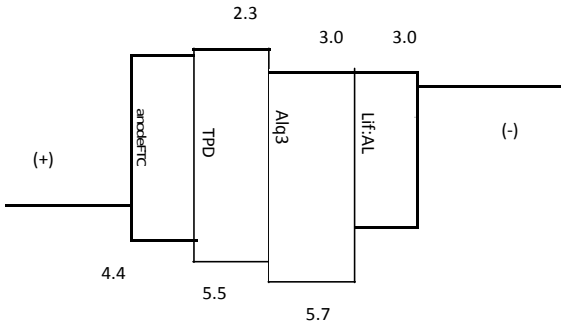

Figure 1 shows the energy band structure of OLED and fig 2 shows the schematic representation of OLED.

TPD and Alq3 films are recorded by UV-double beam spectrophotometer (M ODEL LT 2800) and sheet resistance were measured by four probe set-up. All tests were performed in air at room temperature and under darkroom condition without any encapsulation. All materials are purchased fro m sig ma -aldrich (USA) and used without further purification. The fabricated OLD structures are-

Device (1) FTO/TPD

(10n m)/Alq 3 (15n m)/ LiF(3n m)/Al (120n m)

Device (2) FTO/TPD

(20n m)/Alq 3 (30n m)/ LiF(3n m)/Al (120n m)

Device (3) FTO/TPD

(30n m)/Alq 3 (44n m)/ LiF(3n m)/Al (120n m)

Device (4) FTO/TPD

(50n m)/Alq 3 (70n m)/ LiF(3n m)/Al (120n m)

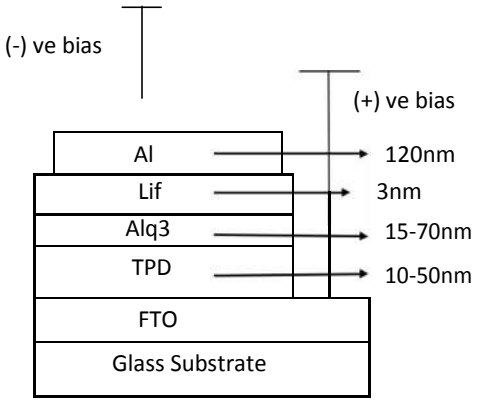

Fig (2): Schematic presentation of OLED

3. Results and discussion

In this work we fabricated the four different sets of bilayer TPD/Alq3 organic thin films with different thickness range and study their transmittance and absorbance (400-700nm) properties with sheet resistance of respected bilayer film in detail. We find that when the thickness of hole transport layer (HTL) and emissive layer (EML) layer is continuously increases, then there is a decreasing tendency of optical property is observed. This implies that optical transmittance is decreases with increasing thickness of respected layer. On the other hand within the range of 30-45 n m thickness of organic layer, device property is suitably enhanced. That is although optical properties are continuously decreases with increasing the thickness of organic layer but the device performance is enhanced within a particular thickness limit. This is due to the higher value of figure of merit (FOM) of the bilayer film, which is an important parameter for study the performance of transparent conducting films. The FOM is defined as FOM= T^{10}/Rs, where T is the optical transmittance and Rs is the sheet resistance [13]. Since higher value of figure of merit indicated the better transparent conducting film, so in our work TPD (30n m)/Alq 3 (44n m) bilayer film provides better result to us. Here luminous intensity becomes more than 2500 Cd/m^2 at this range of thickness. This imp lies that within this limit of thickness, the injection of charge carrier is suitably enhanced as a result of which recombination of electrons and holes takes place more perfectly (i.e. proper balancing of degree of opposition faced by positive and negative charge carrier though the organic layer) and maximum light output will be achieved. Table 1 shows the percentage of transmittance and absorbance value of four different set of TPD/Alq3 bilayer organic films with sheet resistance value at different thickness. The transmittance spectra of these bilayer TPD/Alq3 organic films are plotted against the different wavelength is shown in figure 3.

Serial no	Thickness of TPD/Alq3 bilayer films	Transmittance (%)	Absorbance (arb.)	Sheet resistance (Ohm/square)	Figure of merit (Ω^{-1})
Set 1	10/15(nm)	91	0.0410	18.35	21.22×10^{-5}
Set 2	20/30(nm)	88	0.0555	11.89	23.42×10^{-5}
Set 3	30/44(nm)	83	0.0890	6.37	24.33×10^{-3}
Set 4	50/70(nm)	78	0.1079	4.14	20.18×10^{-5}

From this table it is clear that although the value of surface resistance and optical transmittance is decreased but figure of merit is more enhanced up to the optimize thickness region. After that its value is continuously tend to decreases because of which device performance is reduces. This result verifies earlier report [14].

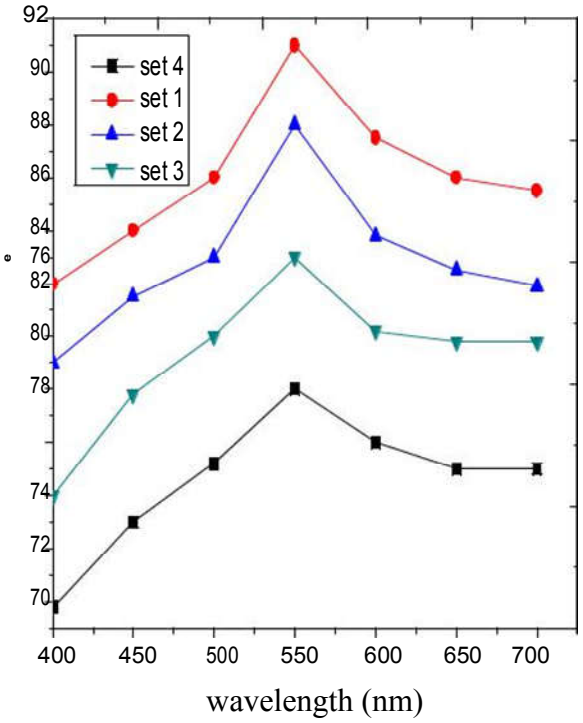

Figure (3): Graph of transmittance and wavelength

Figure (3) shows the spectrum of optical transmittance and wavelength of different set of bilayer organic thin film. From this graph it is clear that transmittance is decreases with the increasing. Similarly figure (4) gives the variation of current density and applied voltage in which device (3) shows the maximum value.

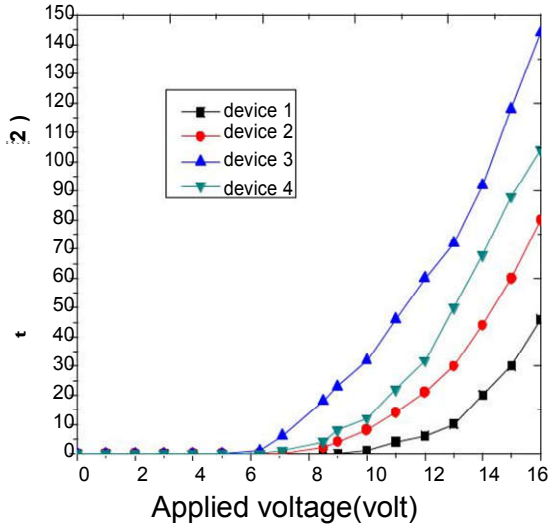

Figure (4): Graph of current density and voltage

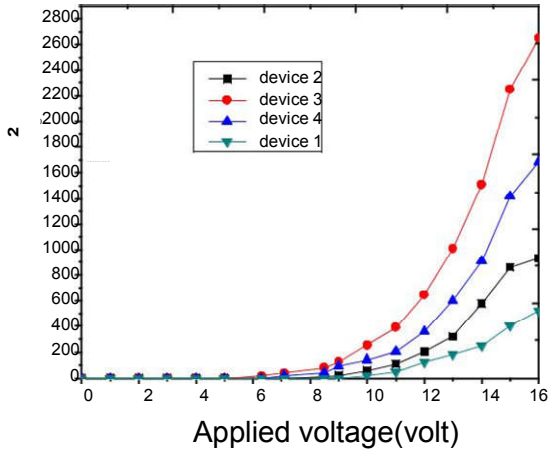

Figure (5): Graph of luminance and voltage

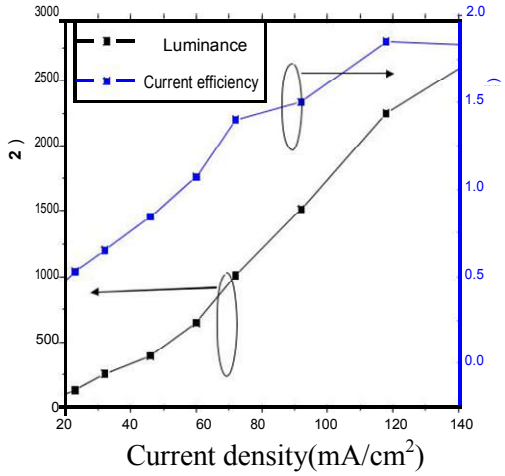

Figure (6): Graph of variation of luminance and efficiency with current density

Here figure (5) shows the graph of luminance and applied voltage in which device (3) gives the highest brightness due to its highest FOM value [15]. On the other hand figure (6) gives the variation of luminance and current efficiency with respect to the current density of the optimized device (3). In this case we obtained the diode characteristics with a turn on voltage less than 8 volt. It is because of the fact that at this range of organic layer thickness film morphology is suitably enhanced due to the decreasing of pinhole density and increasing ordered film pattern within the optimized region of organic layers thickness as we use higher growth rate [16, 17] and also proper balancing of charge carrier injection as mentioned above. Following table 2 shows the property of all the OLED devices in which device 3 shows the better performance compared to other devices.

Table 2: Summary of the property of the OLED devices at different thickness

S.N	OLED devices	Turn-on voltage (volt)	Maximum luminance (cd/m^2)	Maximum current density (mA/cm^2)
1	Device 1	10.12	520	46
2	Device 2	8.50	930	80
3	Device 3	6.71	2650	144
4	Device 4	7.72	1680	104

From this table it is clear that the performance of the device 1 is poor that of the other devices (i.e. low current density and luminance), this may be due to the lack of hole and electron blocking function of organic layer at their too thin film thickness. Because when the thickness is very low then most of the charge carrier simply passed though the organic layer without any recombination leading to low current density and luminance. In our case device 3 received the highest device performance due to proper balancing of degree of opposing force for both the charge carrier along with highest figure of merit (FOM) value.

4. Conclusion:

We have reported a high luminance green OLED with brightness greater than 2500 Cd/ m^2 with turn on voltage 6.7 volt. The structure of the devices has a direct impact on the balancing probability of electron and hole recombination in the emissive region. With larger the thickness of the hole transport layer (HTL) and emissive layer (EM L),

the luminance property is enhanced up to the critical region. We obtain the maximum value of luminance (2650 Cd/m^2) at the optimal thickness of 30 n m and 44n m for TPD and Alq3 layer respectively with current density 144 mA/cm^2 and luminous efficiency 1.80 Cd/A.

5. References:

1. S.Karg, J.C.Scott, J.R.Salem and M .Angelopoulos*,"Increased brightness and lifetime of polymer LED with polyaniline anodes",* Synth.M et. 80,111, (1996).
2. J. Gao, A.J.Heeger, J.Y.Lee & C.Y.Kim, *" Soluble polypyrrole as the transparent anode in polymer LED" ,*Synth. M et.,82,221-22, (1996).
3. G.Gustafsson, Y.Cao, and G.M .Treacy *, Nature,* 357, 477, (1992).
4. Friend R H, Gymer R W, Holmes A B, Borroughes J H, Marks R N and Taliani C, *"Electrolumiance in conjugated polymer ", Nature (London),* 397, 121-8, (1999)
5. *Dodabalapur Ananth " Organic light emitting diode*", Solid state Commun., 202 (2-3), 259-67, (1997)
6. Tang & Vanslyke, *"Organic electroluminescent diode",* Appl. Phys. Lett., 51 (12), 913, (1987).
7. Haichuan M u, Hui Shen and David Klotzkin*,"Dependance of film morphology on deposition rate on organic electroluminescent devices"* , Solid State Electronics, 48, 2085-2088, (2004).
8. N. Thejo Kalyani, S.J.Dhoble and R.B.Pode, *" Fabrication of red OLED using $Eu_xY_{(1-X)}(TTA)_3$ Phen organic complexes for solid state lighting",* Adv. M at. Lett., 2(1), 65-70, (2011).
9. G.Luka,*" Journal of Applied Physics*" 108, 064518, (2010).
10. L.Zhou, J.Y.Zhuang, S.Tongay, W.M .Su and Z.Cui*, "Performance improvement of OLED with aluminum buffer layer for anode modification"*, Journal of Applied Physics", 114, 074506, (2013).
11. Ali Kemal Havari, M ustafa Can, Serafettin Demic, M ahmud Kus and Siddik Icli *" The performance of OLEDs based on sorbital doped PEDOT:PSS"* Synthetic metal (2011).
12. Adriano R. V.Benvenho, Jose P.M .Serbena,vRudolf Lessmann and Ivo A.Hummelgen, *"Efficient OLEDs with FTO anode and electrochemically synthesis sulfonated polyaniline as hole transport layer"* Brazilian Journal of Physics, 35(2005).
13. G. Haacke *"New figure of merit for transparent conductors*" J. Appl.Phys., 47, 4086, (1976).
14. Jianfeng Li, Lianbing Hu, Jun Liu, Lian Wang, Tobin J.M arks *"Indium tin oxide modified transparent nanotube thin films as effective anodes for flexible organic light-emitting diodes"*, Applied Physics Letter, (2008).
15. Jianfeng Li, Lianbing Hu, Jun Liu, Lian Wang, Tobin J.M arks *"Indium tin oxide modified transparent nanotube thin films as effective anodes for flexible organic light-emitting diodes",* Applied Physics Letter, (2008).

16. Zhou X, He J, Liao LS and Lu M , *"Real-time observation of temperature rise & thermal breackdown process on organic LED"*, Adv. M ater, 12, 265-9, (2000).

17. Burrows PE, Bulovic V, and Forrest SR, "*Reliablity & degradation of organic light emitting devices",* Appl. Phys. Lett., 82 (16), 2580-2, (2003).

Si Orientation Dependent Release of SiO_2 Microcantilevers by Wet Chemical Etching Method

Sagnik Middya[1], K. Prabakar[2]

[1]4th Year Student, Department of Electronics and Electrical Engineering,
Indian Institute of Technology, Guwahati - 781039, Assam.

[2]Electronics and Instrumentation Section, Surface and Nanoscience Division,
Indira Gandhi Centre for Atomic Research, HBNI, Kalpakkam-603102, Tamil Nadu.

(*Submitted* 11-05-2017)

Abstract

In this study, fabrication of SiO_2 Microcantilevers (MCs) using wet anisotropic etching technique is reported. Thermally grown SiO_2 (300 nm) layer on single crystalline(*c*-) Si is utilized for the micro-fabrication. Standard lithographic procedure was followed and the exposure of the photo-resist was performed by mask-less direct laser writer. Various orientations on the *c*-Si wafer, their properties and implications on the structure and integrity of the released SiO_2 MC are discussed. The <110> direction was found to be much time consuming and sticking of the released structures was almost evident. On the other hand <100> and <410> directions showed lesser release time and higher stability of the released structures due to under-etching along the width of the MCs.

1. Introduction

Microcantilever (MC) is a simplest mechanical stucure (fixed-free beam) in micro-domain and can be visualized as a miniaturized counter part of a diving board. When specific molecules are adsorbed on its surface, MCs can act as a physical, chemical or biological sensor by detecting changes in its bending magnitude or vibrational frequency [1]. These sensors have several advantages over the conventional ones in terms of high sensitivity, quick response, low analyte requirement, low cost etc., Use of MCs as a mechanical device was actually initiated by Nathanson et al. [2] when they used metal plated MCs as the gate electrode of resonant gate transistor. Surface probe microscopy (SPM) is by far the best example of its application. By the virtue of its well established micromachining techniques and other unique properties, Si stands out to be the most suitable candidate for MCs at a length scale of few tens or at most hundreds of μm. Apart from surface probing, these cantilevers are often used as chemical (in itself or by using a layer of some specific material), [3,4,5] pressure [6] or thermal (utilizing coefficient of expansion) [7] sensors. Piezo-electric or other actuation principles coupled with MCs makes them high end actuators. Similar principle can be extended to develop energy harvesters [8]. Several other possible applications of MCs in the form of heaters [9], humidity sensors have been reported [10]. In the past years, SiO_2 has been found to be an alternative for Si and many SiO_2 based MC systems have been fabricated for a variety of applications [11,12]. Simulations show that for the same load, SiO_2 MCs register a greater bending as

compared to Si MC [13]. Hence SiO_2 MCs prove to be very useful for many practical purposes.

In this work, we present the results of Si crystalline orientation dependent fabrication of SiO_2 MCs by direct laser writer and wet anisotropic chemical etching process.

2. Experimental section

Experiments were conducted on 2 x 2cm cut, *c*-Si(100) wafers with 300 nm thermally grown SiO_2 on both the sides. Fabrication started with standard Si wafer cleaning using standard *Radio Corporation of America* developed *RCA1, RCA2* and *Piranha* solution (3:1 mixture of H_2O_2 to H_2SO_4). The wafer pieces were rinsed in acetone ($(CH_3)_2CO$) and isopropyl alcohol ($(CH_3)_2CHOH$) to remove any organic contaminants after it was brought into clean room. It was placed on hot plate at 100°C for a minute to remove the moisture. Then positive S1818 photoresist was spin coated. Thickness of 1 µm and was confirmed by non contact profiler (Dektak) measurement. Subsequently, it was heated at 65°C (pre-baking) for about 1 minute to evaporate the solvents in photoresist.

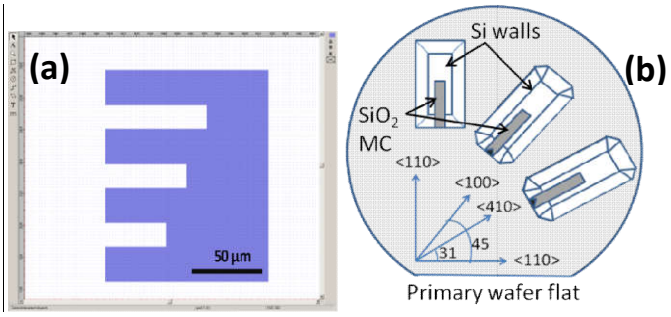

FIG 1: (a) Design of microcantilever array in CleWin Software (b) Different crystallographic orientations and microcantilevers in Si <100> wafer with respect to primary flat.

A design consisting of individual MCs and MC arrays of various dimensions were created using CLEWIN software. A particular design of one such MC array is shown in figure 1(a). The MCs (represented by white projections in the figure) had dimensions of 75 µm, 60 µm and 45 µm. The pattern consists of MCs aligned to three crystallographic orientations of Si namely <100>, <110> and <410>. A schematic representation of these three directions on a <100> Si wafer with respect to the primary wafer flat is illustrated in figure 1(b).

Usually in photolithography, the photoresist is flood-exposed by UV light through a mask containing the pattern. The exposed photoresist region either becomes soluble (positive photoresist) or insoluble (negative photoresist). Here a mask-less technique was adopted. The patterns were transferred onto the photoresist coated wafer using a Direct Laser Writer (LW 405B, M/s Microtech, Italy). The instrument raster-scans a laser beam (wavelength 405 nm) with variable spot size. There is also a provision for auto-focusing the laser beam before executing each scan. Suitable laser power and the patterns are selected from the user console. The spot size can be varied by choosing between different lenses. In our case, a laser power of around 10 mW and spot size of 2 µm was chosen. After exposure, the pattern was developed in CF60 developer for about 45 seconds followed by an immediate dip in deionized water. Every pattern developed was observed under microscope and if found under developed, was kept in developer for few more seconds or if over developed, photo resist was stripped and lithography was repeated. Once the patterns were satisfactory, the wafer was post baked at 120°C for 15 minutes for hardening of the photoresist.

The pattern was transferred from photoresist to wafer, by etching SiO_2 using buffered HF (100 gm of NH_4F, 150 ml of DI water (V) with (V/3) of HF). This gives etch rate of about 300 nm/min. Complete removal of the oxide can be noticed when the hydrophilic oxide turns to hydrophobic nature of the underlying Si. The residual photoresist was stripped in acetone and isopropyl alcohol. Si exposed through the SiO_2 hard mask was etched in the present work to release the SiO_2 cantilever using KOH (potassium hydroxide).

KOH is an anisotropic etchant of Si. Selectivity of KOH etching to crystallographic orientation is <100> : <111>: 66:1 and selectivity against oxide is greater than 200. In the present experiment, 40 % aqueous KOH was chosen as the etching solution. The solution was taken in non interacting alumina crucible and was heated to 75°C (etch rate of 45 μm/h). After the etching process, the etched wafers were removed from the solution and thoroughly rinsed with deionized water without the application of any procedure for the prevention of cracking or stiction of the released MCs. The released MCs were allowed to dry in ambient air and were characterized using optical microscope.

3. Results and discussions

The crystallographic orientation of Si plays a major role while releasing the SiO_2 MCs using chemical wet etching. There are two important aspects, etch time and stability of the released MC which need to be considered. It is well known that Si has a diamond cubic structure and its anisotropic etching behaviour strongly depends on the crystal orientation. For example, the {111} planes are most resistant to etching due to high density of atoms and hence in majority of the cases they form the boundary for the etched structure. To achieve {111} walls, the pattern edges must be in the <110> direction, which is also the direction of the prime flat in Si <100> wafers. The family of {100} planes in Si posses fourfold symmetry and their anisotropic etching can produce either vertical {100} walls or sloping {110} or {111} walls, inclined at 45° or 54.7°, respectively [14]. Similarly, the sectional line of a {411} and a {111} plane points in the <410> direction, forming an angle of 30.96° with <110> direction. These orientations and their relative directions are shown in figure 1(b). These orientations determine the way etching of Si below the MCs progress which in turn impacts their properties.

Figure 2 illustrates an optical image of <110> oriented partially released MCs (parallel to primary wafer flat). Bound by slow etching {111} planes, it is difficult to etch below the MCs along these directions. Etching starts once some fast-etching planes are exposed at the convex corners and progresses along the length of the MC [14], known as frontal under-etching. As an outcome, releasing times of MCs are dependent on their length and the structures tend to be unstable. In this process there is also a possibility that the MCs bend and get stuck to the floor of the etch-pit. Figure 2 depicts the progress of under-etching as well as the length dependency of etch-time. While the smallest MC has been released completely, the others are yet to be released. It may be noted all the MCs released in the present work, appear transparent under optical microscope because of the ~300 nm thickness of SiO_2.

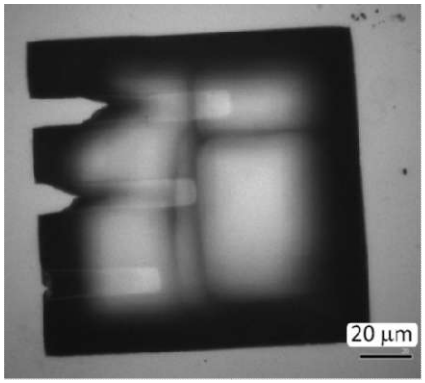

FIG 2: Optical image of array of Microcantilevers along <110>. The SiO_2 MCs appear transparent. The smallest MC has been released while the others are yet to be released.

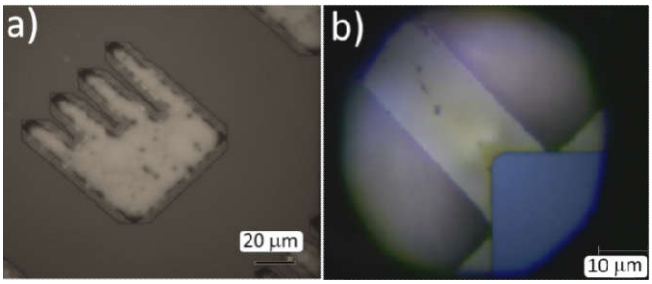

FIG 3: Optical images of <100> oriented MC a) yet to be completely released microcantilevers and b) showing symmetrical triangular projection of {111} Si planes at the fixed end of the completely released microcantilevers.

In the <100> direction, both {100} and {110} planes are present. If KOH is chosen as the anisotropic etchant as in our case, the Si projections below the unreleased MCs are bounded by {100} planes resulting in vertical walls. This can be justified by considering that {110} planes etch faster than their {100} counterparts in KOH solution. Both the {100} and {110} planes can be etched quickly and hence under-etching proceeds laterally i.e. along the width of the MCs as indicated in figure 3(a). As a consequence, MCs require less time to be released. The release-time depends on the width and is almost independent of the lengths of the MCs. As under-etching proceeds along the width, the gradually thinning line of Si acts as a support for the MC thus preventing it from collapsing [14]. Figure 3(b) shows that even on complete release, there is still a symmetrical triangular projection of {111} Si planes at the fixed end of the MCs. This happens because {111} planes are relatively etch-resistant.

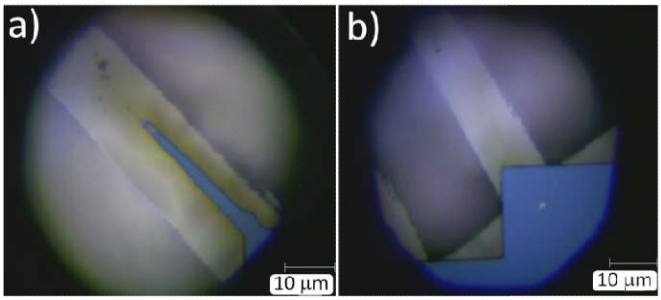

FIG 4: Optical images of <410> oriented MC a) yet to be released and b) completely released and showing unsymmetrical triangular projection of {111} Si planes at the fixed end of the MC

As mentioned earlier, the fast-etching {411} plane intersect the {100} plane (also the wafer surface) along the <410> direction inclined at 31˚ with respect to the primary flat. Thus, the MCs oriented along this direction are released by under-etching of {411} planes. This direction also exhibits some sort of lateral under-etching (Figure 4(a)) though not uniform on both sides as in case of <100> direction. Much like <100> direction, here we also observe a triangular projection of {111} Si planes at the fixed end of the released MCs. However, as figure 4(b) illustrates, in this case it is unsymmetrical. As mentioned earlier in the context of <100> direction, this lateral under-etching feature has the advantage that the released MCs are stable. A comparison between various MCs released in the present work is given in table 1.

As a summary, in the present study, SiO_2 micro-cantilevers of various dimensions and crystallographic orientations were fabricated on Si by wet chemical etching method. The released MCs where characterized using optical microscope. It is found that the release time of MCs oriented in the direction of <100> are dependent on their length due to the frontal etching. Hence for an array consisting of different dimensions of MCs, at any point of time the already released MCs have a greater chance of collapsing or sticking with the bottom.

Direct-ion	**Angle**	**Remarks on released MCs**
<110>	0˚	1. Frontal etching 2. Release time depends on MC length 3. MCs are unstable 4. Shortest MCs are completely released. Some MCs tend to stick to the bottom
<100>	45˚	1. Lateral etching 2. Release time is independent of MC length but depends on its width 3. MCs are stable 4. Though the MCs are released, there is a symmetrical triangular projection of Si below the fixed end of MCs
<410>	31˚	1. Lateral etching 2. Release time is independent of MC length 3. MCs are stable 4. MCs are completely released, but unlike <100>, the projections of Si below the fixed end of MCs are unsymmetrical

TABLE 1: Orientation of Si wafer and properties of the released SiO_2 MCs along those directions. Angle is with respect to primary flat of the Si <100> wafer used.

Whereas, in the case of MCs oriented in the direction of <110> and <410>, the release time was independent of its length because of lateral etching. Quite intuitively these structures are more stable as a thin line of Si remains below the MC throughout the vigorous etching process until it gets dissolved. It can be concluded that in spite of the remnant triangular Si projection at the fixed end of the MCs, the <110> and <410> direction shows better resilience to fabrication.

4.Acknowledgements

Authors thank Mr. Raghuramaiah, EIS, MSG, IGCAR for useful discussions.

5. References:

[1] S K Vashist, " A Review of Micro cantilevers For Sensing Applications", J nano technology, **2007**, 3, 1.

[2] Z H. C. Nathanson , W. E. Newell, R. A. Wickstrom, and J. R. Davis Jr., *IEEE Trans. Electron Dev.* **1967**, *ED-14*, 117.

[3] K. M. Goeders, J. S. Colton, and L. A. Bottomley, *Chem. Rev.* **2008**, *108,* 522.

[4] N. V. Lavrik, M. J. Sepaniak, and P. G. Datskos, *Rev. of Sci. Instru.* **2004**, *75*, 2229.

[5] F. M. Battiston, J. P. Ramseyer, H. P. Lang, and M. K. Baller, *Sensors and Actuators B: Chemical,* **2001**, *77*, 122.

[6] S Bianco, M Cocuzza, S Ferrero, and E Giuri, *J. Vac. Sci. & Technol. B* **2006,** *24*, 1803.

[7] W. Fang, H. C. Tsai, and C. Y. Lo, *Sensors and Actuators A: Physical,* **1999**, *77*, 21.

[8] S. R. Anton, and H. A. Sodano, *Smart Materials and Structures,* **2007**, *16*, 1284

[9] J. Lee, T. Beechem, T. L. Wright, and B. Nelson, *J. of Microelectromechanical Systems*, **2006**, *15*, 1644

[10] S. Chatzandroulis, A. Tserepi, and D. Goustouridis, *Microelectronic* **2002**, *61*, 955

[11] Y. Tang, J. Fang, X. Yan, and H.-F. Ji, *Sensors and Actuators B: Chemical* **2004**, 97, 109

[12] V. Chivukula, M. Wang, H. F. Ji, A. Khaliq, and J. Fang, *Sensors and Actuators A* **2006**,*125*, 526

[13] R. Ab. Rahim B. Bais, and B. Y. Majlis, *ICSE 2008 Proc.,* Ed. Johor Bahru, Malaysia **2008**, 21

[14] V. Jović, J. Lamovec, M. Popović and Ž. Lazi *J. Serb. Chem. Soc.* **2007,** *72*, 1127